

Author response

The authors would like to thank both reviewers for their very constructive comments. We are glad to see that the reviewers appreciate the scope of our work, but we acknowledge that the issues raised are very important and need to be addressed to improve the quality of the manuscript. The most important changes are the addition of two new figures, a substantial revision of Sec. 2.2 and Appendix A, the addition of new Discussion section, and the removal of Appendix B. Below we present our response to all reviewer comments in blue.

General minor remark

A typo had occurred in Table 1. The value of the exchange coefficient Γ_T should have exponent -3 instead of -5. This has been changed.

Response to Reviewer 1 (Tore Hattermann)

General comments

The manuscript under review presents a new approach to parameterize the spatially resolved basal mass balance beneath floating ice shelves. The applied method uses the scaling of basal melt rates as a function of geometrical parameters and ambient ocean temperatures that has been derived in previous studies from a one-dimensional inclined plume model. Validation of this parameterization for the one-dimensional case is given through direct comparison with the underlying plume model. Aiming at generalizing the approach for two-dimensional applications, algorithms are proposed to compute local geometrical input parameters for an arbitrary ice shelf geometry. To evaluate the method, circum-Antarctic melt rates are computed by tuning the ambient ocean temperatures to reproduce realistic area averaged melt rates and subsequently comparing the associated spatially resolving melt patterns with maps of observed basal melting.

The authors convincingly show that their method provides a significant improvement compared to the two referred simplistic approaches of Beckmann and Goosse (2003) and DeConto and Pollard (2016) that scale basal melting solely based on the temperature difference between the ambient ocean and the local freezing point. While following directly from a model of the underlying physics, the method is of general nature and (presumably) contains few enough free parameters to prevent over-fitting. Based on this, the presented work is inevitably a sound and useful contribution for better understanding and modelling ice-ocean interactions and should be published.

Thank you for the positive words and for acknowledging the merit of our work.

Said this, the following three concerns need to be addressed to make the merit and scope of this work fully available to the reader.

1 - The origin of the general melt rate curve needs clarification.

In the present manuscript, it is unclear how this central element of the parameterization was obtained and to which extent its derivation has been part of the current study and how much is based on previous works. Although not being explicitly mentioned, an expression of the curve shown in Fig. 2 seems to be given in eqn. A3, but also here lacking a proper derivation or a reference thereof. Meanings of the individual terms are discussed in the text, but neither their exponents nor the fact that they should be multiplied including the factor 10. A more explicit description of what has been done (and by whom) to establish this relation is needed. To ease the line of argument, it would probably also be useful to add a summary of the nature of the basal melt parameterization found by Jenkins 2014 (i.e. the existence of a general melt rate curve) at the beginning of section 2.2., e.g. by moving the paragraph on p. 8, l. 6-14 up front, including eqn. A3, and stating that the remainder of the section will review the meaning of the respective terms.

It is correct that some of the details of the plume parametrization have only been shown in the conference contribution by Jenkins (2014). We have tried to summarize the most important aspects as best as possible, but obviously this was not clear enough. We apologize for the confusion. One of the reasons to keep this summary rather concise is that a second paper is planned that discusses the derivation of the plume parametrization in full detail. To overcome this gap, we have reformulated most of Sec. 2.2 and added some new details in Appendix A. One aspect to keep in mind is that the current parametrization is ultimately based on a purely empirical study of the plume model results. The original scaling found in Jenkins (2014), including coefficients and exponents, was not derived analytically but empirically. We have now added some analytical results to the Appendix that (partially) justifies where the mathematical form of the equations comes from. We hope to further extend this analysis in a different paper.

We are grateful for the suggestion to move the final paragraph of Sec. 2.2 to the front. This indeed clarifies the form of the parametrization before the details are discussed.

For clarity, we would like to stress that eq. A3 is strictly speaking *not* the equation describing the curve in Fig. 2, but the equation describing the melt rate scale. The curve in Fig. 2 is the *dimensionless* curve obtained after scaling and described by the polynomial coefficients in Tab. A1. Hopefully this has been clarified in the newly formulated Sec. 2.2.

2 – The rationale for the extension of the general melt rate curve for the two-dimensional case needs to be explained and discussed.

A basic assumption of the underlying plume model is that the geometry of the ice shelf is uniform in the direction perpendicular to the plane in which the plume is rising (p. 4, l. 15-16). This leads to a system of one dimensional equations (p. 5 l. 6-12) that yields the general melt rate curve when being evaluated for the parameter space of interest. One restriction that is imposed by this one-dimensionality and that is inherit to the general melt rate curve, is that changes

in plume thickness and hence the susceptibility of relevant properties (such as plume temperature and buoyancy that in turn controls its speed) are fully predicted by the sum of the fluxes through the upper and lower interface with the ice and ambient ocean respectively. For a two-dimensional configuration, however, one would expect that the width of the plume becomes a dynamic variable of some sort, which through mass conservation affects the plume thickness as well as the width of the interface through which the plume interacts with the ice and ambient ocean. The result would be an increased degree of freedom and I am inclined to believe that this would lead to significant deviations from the general melt rate curve found for the one-dimensional case. This issue is currently lacking attention in the study.

For instance, many ice shelves exhibit asymmetric geometries, being narrower towards the grounding line and wider towards the ice shelf front, as simplistically illustrated in fig 1. Considering that every point of the ice base is covered by a multitude of plumes arising from the deepest grounding line, it is obvious that each individual plume must become wider (and hence thinner) as it ascends towards shallower depth, with direct consequences for its evolution. In fact, augmenting the original plume model of Jenkins (1991) by implementing a varying plume width in a two-dimensional configuration (Hattermann, 2012 section 3.5) it is possible to reproduce melt rates obtained from a general circulation ocean model of a realistic ice shelf geometry for a range of forcing parameters (Hattermann, et al 2014), while for the same setup, the original plume model is overestimating the melt rates along a one-dimensional flow line by an order of magnitude, primarily because the unscaled (for width) plume predicts too vigorous currents beneath the shallower part of the ice shelf. In essence, the extension into two-dimensions is likely to weaken the influence on the non-local effective grounding line depth, as a thinner and wider plume would more quickly cool and slow down on its rise along the ice base, remaining less of its properties at the source location (possibly also earlier reaching ambient buoyancy and detaching from the ice base, leading to initialization of a new plume at the detaching depth—a case that is not discussed in the manuscript at all).

Much effort has been spent in the current manuscript on reviewing the one-dimensional plume theory that is the basis of the generalized melt rate curve. However, it is currently lacking a discussion and evaluation of the validity of the transfer of that relationship and its underlying physics to higher dimensions and the possible shortcomings therein, such as the above mentioned consequences of mass conservation for an asymmetric distribution of ice shelf area with depth (which is a qualitatively different argument concerning the plume physics than the fact that there might exist multiple plume pathways). I acknowledge that this assessment can be added at various level of detail. Also, in the overall need for simplicity and recognition of other examples of parameterizations that have been used in the past, the presented approach is likely to be justified as is for the purpose of providing boundary conditions for ice sheet models. But the authors need to add some sort of assessment of physical basis for their transfer, which appears to me the major advance of this study.

We fully agree that the one-dimensional formulation of the plume model is a rather strong assumption and regret not having spent more attention on this issue, so we take the opportunity to discuss this briefly. A discussion of the neglected two-dimensional effects including the references mentioned above has been added to Section 2.3 and the Discussion section. However, we hope that the reviewer realizes that the current approach is nothing more than a parametrization of the net circulation within the cavity, which can never fully capture all the physics. Still, it would be interesting to explore this and other extensions of the plume model in a later stage.

3 – The evaluation of the performance of the parameterization for the circum-Antarctic case needs improvement, in particular, more information must be provided on the limitations and processes not captured by the present approach.

In the current manuscript, the performance of the method is evaluated by comparison with the simplistic approaches of Beckmann and Goosse (2003) and DeConto and Pollard (2016). In particular, the generalized plume approach is shown to be largely superior in reproducing a qualitatively realistic spatial pattern of basal melt (increased melting towards the grounding lines) and the need of fewer adjustments of the ambient ocean temperature field to obtain spatially averaged melt rates that match the observations than required by the traditional thermal driving parameterizations. From an ice dynamical modelling perspective, this is certainly an important step forward. However, today, models of a wide range of complexity are used to assess the ice-ocean system (see e.g. Asay-Davis et al., 2016 for a summary) and within the scope of these works, it is desirable to evaluate the proposed parameterization also with results from the other end of the spectrum. A couple of circum-Antarctic ocean general circulation models are readily available (even more regional models, some of already coupled with ice models), providing fields of basal melt rates by explicitly resolving the ice shelf cavity circulation. Although not necessarily yielding realistic results everywhere, all of these simulations provide a self-consistent sets of geometrical parameters and ambient ocean temperatures that can be used to scrutinize the validity of the presented plume parameterization. Applying the new parameterization in the context of a fully resolving ocean model framework of the author's choice appears to be a minor additional effort and I highly recommend that such a comparison is added to this publication, as it would substantially aid the validation of the approach (such as its extension to two dimensions) and greatly improve the understanding and integration of the new method within the context of existing works on simulating basal melting.

We agree that evaluating the basal melt parametrization in the context of an ocean general circulation model would be a necessary step for the validation. This is certainly one of the goals that one should work towards. However, we think it would be too ambitious for the current paper and it is not clear if it is as easy as the reviewer claims. The current paper focuses on the evaluation of the melt rates for a fixed present-day temperature field and geometry. Although using an ocean model for determining the ocean temperatures might be less ad hoc than extrapolating the observations, such a model also contains many uncertainties and does not necessarily give more realistic values. In other words,

adding the results of an ocean model would require a detailed description and discussion of the ocean model itself, which would make the current work too extensive, losing focus on the parametrization itself. We hope the reviewer agrees that the problem of modelling basal melt rates on these scales is a very difficult one that requires several careful steps. The first step is showing that a plume parametrization can capture more realistic melt rates than the frequently used parametrizations of the Beckmann & Goosse type, even in its simplest form.

Another issue is that the melt rate maps shown in Fig. 10 work well to assess the improvement over the simplistic scaling of DeConto and Pollard (2016), but do not allow to compare the details of the melt rate map with the observations of Rignot et al. (2013) that is used as a reference (p. 20 l. 10-14). In particular, the truncation of the color scale to melt rates of 2 m/yr excludes a quantitative assessment of the maximum melt rates that can be an order of magnitude larger at some grounding lines with important effect on the ice dynamics.

We agree that this can be improved. The colour scales for the figures have been extended to 5 m/yr and a new figure has been added showing the Rignot data and the difference between these data and the parametrization. Furthermore, we have added zoomed panels for 3 important regions with a logarithmic colour scale, so that the assessment of the maximum melt rates is facilitated.

Within this scope, it is currently also not accessible to the reader, how the tuning points for the ambient ocean temperature field were chosen and by which algorithm the temperature in these points has been optimized to match the area averaged melt rates (see specific comments for details).

The description of the method behind determining the effective temperature field has been improved; see also our replies to the specific comments. We also refer to our reply to Reviewer 2, who has more detailed concerns about the ΔT field. In short, we acknowledge that there are many uncertainties present in our constructed temperature field and we have tried to be more critical throughout the manuscript, including the newly added Discussion section.

Eventually, there are a couple of processes that are known to influence basal melting around Antarctic, but are not captured by this parameterization, with examples being the influence of regionally varying tidal current strength on the boundary layer heat exchange (Maksinon et al. 2011), as well as the enhanced heat exchange due to winds (Hattermann et al. 2014, Dinnemann et al. 2015) as well as intrusions of solar heated summer water near the ice fronts (Hattermann et al. 2012, Stern et al. 2013). Hence, their influence must either be omitted or be included in the fitting of the temperature field, a limitation of the new approach that needs to be discussed.

We have chosen to keep a fairly simple parameterization and a key purpose is to use it in ice dynamical models. Nevertheless we will discuss the simplifications we take in more detail and along the lines suggested by the reviewer. Of the effects mentioned above, mode 3 melting (also mentioned by Reviewer #2)

might be the most important one to discuss, so we added these references to the Discussion.

Also, to some extent the precision of language and figure quality should be improved.

Specific comments

p. 2, l. 11 & 15: What kind of "steady-state" is referred to and what is meant by the "steady nature" of the parameterizations? Does the new parameterization differ in a manner that it is time-varying of some sort?

Thank you for this point. The essential difference between the two parametrizations is rather local vs. non-local. We have changed this in the text.

p. 2, l. 14: Please clarify the ambiguous formulation "geometry below the ice shelves".

This has been changed to "geometry of the ice-shelf base".

p. 2, l. 27-28: How does the referred mechanism in which upward flowing plumes induce inflow of warm water into the cavity relate to the approach presented? To my understanding, this possible feedback on the ambient ocean temperatures is not part of the plume model or the derived parametrizations, opposing the subsequent statement in line 32.

Again a good point. This feedback mechanism is indeed not part of the parametrization, but we prefer to mention it here as a brief summary of the physics in the cavity. To avoid the contradiction in the next paragraph, we have changed "All these physical processes" to "The dynamics of the plume".

p. 3,l. 1-2/p. 8,l. 16ff/p. 22,l. 6-8: With the above general comment in mind, please reflect on the validity of the underlying physics, in particular the non-local dependence on grounding line depth, when extending the plume parameterization to two dimensions.

We hope that the additional lines in Sec. 2.3 and the Discussion section address this issue appropriately.

p. 3, l. 15-18: It is not always clear, which parts of these sections review the results of previous works and which parts are original contributions of the present study. It is mentioned that results are summarized from Jenkins (2011) and Jenkins (2014), while particular advances of the present study are not discriminated in detail. To some extent, the problem may arise, because a central reference of the plume theory is contained in a conference presentation, which is not available for reading. However, explicitly clearly labeling review information and original material of this paper at the beginning of the subsections, should sufficiently mediate this issue.

As explained in our reply to major comment 1, we fully agree that it is an issue that the details of the parametrization have only appeared in a conference contribution. Hopefully, our revision of Sec. 2.2 and Appendix A has resolved this issue. The main original contribution of this paper is the extension of the parametrization to 2-D. We tried to clarify this at the start of the subsections. It might be important to note again that the added analytical solution of the simplified plume equations (Appendix A) has not appeared in Jenkins (2014) and can also be considered a new contribution of the current manuscript.

p. 4, l. 3-5: It would be useful to explain how the ocean current that drives mixing relate to the temperature, hence leading to the non-linearity referred to here. Does this refer to the effect of increased buoyancy by decreased salinity due to more meltwater input for higher temperatures?

We added an additional reference to Holland et al. 2008, where this is explained in full detail. The crucial element is indeed the linear temperature dependence of the ocean current.

p. 6, l. 8: For clarity, mention which simplification is applied, i.e. the assumption of a constant ratio between Γ_T and Γ_S .

Thank you for noting this; we have added a sentence that explains it.

p. 6, l. 23 ff.: The derivation of the general melt rate curve appears somewhat fragmented and I am currently not able to retrace its origin based on the information given in this section. In particular, it is not clear how the terms in eqn. 7 to 9 combine into a single expression. Specifically, it is unclear how Jenkins' extension of eqn. 7 looks like and what is described by the universal length scale mentioned on p. 7, l. 21 or how it is used. Also the discussion of the two different melt formulations (p.7, l.21-27) is confusing in the given context, as is the summarizing statement in p. 7, l. 28 (amplitude of which curves?!). Clarity would probably be added by stating in the beginning of the section that Jenkins 2014 has derived an explicit and universal expression of melt rates as function of distance from the grounding line (possibly including eqn. A3) and explaining that the remainder of the section revises the basic ingredients, to sketch how the relationship was obtained but without providing a stringent derivation.

As already explained in the reply to the major comments, we have significantly rewritten this section, taking into account your suggestion to show the form of the parametrization at the start and go into the physical meaning of the terms afterwards.

We hope that the discussion of the two melt formulations make more sense in the revised text. The point is that an empirical expression for Γ_{TS} in terms of other quantities is added to complete the procedure for finding the universal length scale. It is one of two extra ingredients for extending the original length scale of Lane-Serff (1995).

The "amplitude of the curves" refers to the plume model results that are scaled by M in order to produce the dimensionless curve in Fig. 2. This has been clarified as well.

p. 8, l. 1 & 2: The plume buoyancy is primarily controlled by salinity, while temperature has only little influence on the density for the given parameter range. Even though this is not stated explicitly, I assume that by parameterizing the plume buoyancy through the temperature difference between the plume and the ambient ocean, an assumption was made on how the temperature difference translates into a salinity difference (i.e. the freshening of the plume is obtained from transforming its respective source water along the melting-freezing mixing line/ Gade line). Does this imply that the general melt rate curve was obtained by assuming that the ambient water at any location along the plume path is the same (or lies along the same Gade line) as at the grounding line where the plume originates? In this case, this would be an important limitation of the theory, which is almost certainly not true for many ice shelves, where different source water types may dominate the ice ocean interaction in different parts of the ice shelf cavity (e.g. different sources of HSSW beneath Filchner-Ronne or the influence of more buoyant surface water near ice shelf fronts).

The revision of Sec. 2.2 and Appendix A should hopefully clarify what the underlying assumptions of the plume parametrization are. It is definitely true that salinity difference are the direct driving mechanism of the plume, and that this is indirectly controlled by the input of meltwater in the plume and, hence, the temperature difference that controls the melting. The theoretical arguments added to Appendix A show how these effects end up being parametrized in terms of the temperature difference alone, indeed under the assumption of constant ambient properties. One can regard this as a limitation, but no parametrization is, of course, able to capture all the physics. In our opinion, this is the simplest way to capture the key physics for producing a net circulation within the ice-shelf cavity. Other effects, such as stratification and different water masses, are certainly important and these should be included and investigated at a later stage. Still, we have added some words about this in the Discussion section.

p. 10, l. 6-12: If my understanding of this algorithm is correct, valid plume paths will also incorporate directions for which the ice base slope reverses somewhere between the given ice shelf point and the respective grounding line since only the local slope and overall grounding line depth are evaluated. What does this imply for the nature and realism of the resulting multitude of valid plume paths?

This is correct. It could be possible to check the slope in between and discard plumes paths for which the slope reverses. But one should keep in mind that this is just a parametrization that is supposed to describe a net circulation. We believe that for the resolution considered here, adding more complexity to the algorithm would have little effect. Yet, it is something that one should look into when considering higher resolutions and more sophisticated plume models, e.g. the 2-D plumes that you have proposed. See also the added lines in the Discussion section.

p. 15, l. 6-9: Should be moved to discussion and supported through proper references.

As discussed in more detail in the reply to Reviewer #2, we believe it was a mistake to mention these models here, because it appears that they are not really used in a proper reference except in our own ice model for testing purposes. These particular sentences have been removed.

p. 16, l. 5: For the given temperature range, the buoyancy of the plume is dominated by salinity differences. Please comment how the uniform salinity field affects the response of the melt rate parameterization (or its inherent ingredients).

Indeed, the main driving mechanism of the plume is the density difference caused by the difference in salinity between meltwater and ambient ocean. As we hopefully clarified in the previous replies and the revision of Sec. 2.2 and Appendix A, the plume buoyancy depends on the difference $S_a - S_i$ (with S_i taken equal to zero) and the temperature differences $T_a - T_f$ and $T - T_f$. The result is that the buoyancy is parametrized entirely in terms of S_a and the temperature difference $T_a - T_f$, which controls the input of meltwater. The bottom line is that the current parametrization does not account for vertical ambient density profiles, and therefore the absolute value of S_a (or more precisely, the relative value w.r.t. $S_i = 0$) only controls the initial buoyancy of the plume at the grounding line, both explicitly and through the freezing point T_f . Horizontal variations in S_a around Antarctica are then much smaller than its absolute value and have a very weak effect on the parametrization output. Of course, this would all change if one would include stratification explicitly. We added a line in the text that distinguishes between horizontal and vertical variations and refers to the Discussion section.

p. 18, l. 9-11: More information on this tuning process must be provided. How were the respective temperature differences in the 29 sample points determined? Presumably, some sort of optimization algorithm has been applied, that involves iterative computation of area averaged melt rates and subsequent adjustment of the individual correction points. How well does this procedure converge towards a unique solution for the given cost function? Why were 29 points used and how have they been allocated and how sensitive is the resulting melt rate map to this particular configuration (from Fig. 10a and Fig. 11a one could get the impression that more spatial detail on the melt rate map correlates with a higher density of correction points)?

We apologize for the confusion here. The 29 sample points have not been determined by a sophisticated algorithm but were chosen by a trial and error. We tried to clarify this in the text. One criterion is to limit the biases near grounding lines resulting from the interpolation between ice shelves (e.g. FRIS). But there are also regions (e.g. Dronning Maud Land) where warm open ocean temperatures are extrapolated into cavities due to the lack of cavity points in the observations. This causes higher values T_0 that would overestimate the melt rates (as we found) and require a negative ΔT .

This is not a unique optimal solution (as we added in the text), but merely a necessary exercise in order to obtain the required input field. See also our reply to Reviewer 2. By his suggestion, we have changed the tone of this section,

clarifying that the method is simply an inversion of the basal melt parametrization, yielding ocean temperatures that are not necessarily realistic. Since ΔT is the result of linear interpolation, we don't expect the melt rates to be very sensitive to the number of sample points. Rather, the melt rates might be sensitive to the *values* of ΔT (see also Sec. 3.1), but this seems a different matter. The current number 29 appears to be around the minimum number of points necessary to obtain the correct *average* melt rates for each shelf group. Adding more points likely has little effect on the average melt rates.

To put it differently, one could also have chosen to "tune" a single effective temperature value for each ice-shelf cavity. The current method aims at obtaining the values from observations and makes the values slightly spatially variable.

The spatial variation in the melt rate maps *within a cavity* is really a property of the parametrization itself, as we showed in Sec. 3.1. Of course, the spatial variation over the entire domain is related to the temperature field as well, but this is the aim of the construction.

We also added a few lines about this to the Discussion section.

p. 18, l. 24-27: It is well known that most of the seawater beneath the FRIS is significantly colder than the surface freezing point. The reason for this is that melt water produced at greater depths is largely recirculated within the cavity and mixes with inflowing water at the surface freezing point, before this interacts with the ice base. Thus a representation of colder ambient water masses would indeed be more realistic in this case.

This might indeed be one of the reasons why the melt rates under FRIS are overpredicted. However, there are two things one should take into account here. First, we only use the annual mean of the temperature observations (we apologize for not clarifying this earlier), so the coldest temperatures are likely not present in the effective temperature field. Second, the plume parametrization in its present form essentially only describes a net circulation with (ideally) a single length scale (hence a single ambient temperature) per cavity. The ambient temperature in this sense represents the net inflow into the cavity and not the temperature of melt water that is produced or mixed locally. We have added some lines in the Discussion section about this. Still, the parametrization clearly does not reproduce the situation under FRIS in a satisfying way. Also note the comments of Reviewer 2 about relaxing the lower bound for the effective temperature.

p. 18, l. 32-33: In fact, the continental shelf temperatures in West Antarctica in Fig. 8a appear rather low compared to observed values well above 0 degC. It would be useful know more about the spatial pattern of basal melt in this region and its comparison compares, in particular if the parameterization is capable of capturing the extremely large melt rates near the grounding lines that are observed here.

Fig. 8a is obtained directly from the WOA13 observations, which do not seem to contain these temperatures above 0 degrees. Maybe the confusion is caused by the fact that we used annual mean data. This is clarified in the caption. Also note

that the ΔT values in West Antarctica (circles in Fig. 8b) are all positive, so the effective temperature used for calculating the melt rates will be higher than the values of T_0 here. As far as the spatial detail is concerned, we have added an additional figure to Sec. 3.3 that should clarify this.

p. 21, l. 5-14: Obviously, the new plume parameterization provides significantly improved spatial basal melt patterns compared to the simplistic temperature scaling. However, to this end, it remains somewhat unclear to what extent the obtained spatial pattern of basal melt is a result of underlying dynamics of the parameterization or reflects the optimization of ambient ocean temperatures that were used for the input.

As discussed above, the spatial variation within a cavity is an inherent feature of the parametrization, which is clearly shown in Sec. 3.1. On the other hand, the melt rates can indeed be rather sensitive to the ocean temperatures (also shown in Sec. 3.1).

Thus, a direct comparison with melt rates from a more comprehensive ocean circulation model remains a desired complement to round off the present study. This, to my mind easy achievable extension of the present work would both help to justify the ad hoc extension for the two dimensional case and scrutinize the predictive capacity of the parameterization that is required for using it in a framework of evolving ice geometry or ocean temperature sensitivity studies.

We appreciate the suggestion, but as already mentioned in our reply to the major comments, we are not sure if the suggested additional study with an ocean general circulation model is as easy as the reviewer claims. The current study is meant to show how the plume parametrization in its simplest form behaves when applied to all Antarctic ice shelves. The construction of the necessary ocean temperature input field is indeed an important uncertainty, but the results from an ocean model would not necessarily be more realistic. A carefully developed sensitivity experiment would be required to introduce this coupling, which can be the topic of an entire follow-up study. Nevertheless, some lines about this issue have been added to the Discussion section.

p. 23, l. 3-7: In addition to the prescription of valid plume paths provided in this study, an extension of the one-dimensional plume theory to higher dimensions needs to account for the effects of mass conservation when the dynamical equations are not constrained along a path of uniform width. This will have consequences on the validity of the general melt rate curve that need to be addressed here.

As noted before, this issue is now addressed in Sec. 2.3 and the Discussion section, while parts of the Conclusion section have been toned down.

Figure 4: Use different colors for open ocean and land areas where the relevant fields are undefined.

It turned out to be difficult to add different colours for the land and ocean areas in Matlab. As a compromise, we made both areas white and drew the contours of the borders between the 3 mask areas, as was done for Figs. 10 - 13.

Figure 1: Extend range of melt rates, consider using non-linear color scale.

(Assuming that this refers to Figs. 10 - 13) The color scale has been extended to +/- 5 m/yr so that it becomes easier to compare directly to the Rignot data, which we also added (see the new Fig 12). We considered a non-linear color scale, but this appears to lower the overall contrast between high and low melt rates rather than highlight the highest melt rates. However, we did use it for the new zoomed figure (see below).

Generally, most spatially resolving circum-Antarctic fields are difficult to assess. Consider the use of zoomed inlets to magnify relevant regions.

A new figure was added (Fig. 11) with three panels zooming in on FRIS, West Antarctica and Ross, respectively. The colour scale is logarithmic and essentially only shows the positive regions (negative and zero values have been made white). Coming back to your previous remark, Fig. 11b shows now that the melt rates around Pine Island and Thwaites have an order of magnitude of 10 m/yr. Although these values are quite high, they are not as extreme as the values of 50-100 m/yr found locally in Rignot data. A remark about this was added to the text.

Technical corrections

Generally, the manuscript should be edited to improve the precision of language, including the removal of unnecessary conjectures and filling terms (examples being p. 1, l. 23: "Therefore", p. 4, l. 13: "ultimately", p. 7, l. 13: "hence", p. 8, l. 6: "thus", p. 9, l. 12: "easily", p. 9, l. 14: "Now", p. 11, l. 1: "In summary", p. 13, l. 16: "clearly", p. 18, l. 30: "Clearly", p. 20, l. 7: "obviously", p. 20, l. 20: "immediately") as well as first person narratives which is extensively used throughout the manuscript.

Most of the suggested corrections have been applied, though sometimes we think that these words are useful for aiding the reader. The first-person narratives have been changed only in a few instances. We do not really agree that this form is used too extensively. It is a style that is widely used nowadays in scientific articles, and changing everything to passive voice does not necessarily make the text easier to read or more objective.

p. 1, l. 20: "ocean flow", better use "oceanic heat supply"

Maybe "oceanic heat exchange" is even better?

p. 2, l. 3: "In the view of these issues", imprecise, clarify: "In order to correctly predict the evolution of the ice sheet"

corrected

p. 3, l. 6: "An important part of this work is [the derivation/ the development of] an algorithm"

corrected

p. 3, l. 25 & 24: consistently refer to "sea water" when introducing rho_w and c_w.

corrected

p. 6, l. 2: if only similar, what is the difference between eqn. 1b and 5c.?

"similar" has been changed to "equivalent". The difference would somehow be the salinity (Sw or Sb), but the equation itself is of course the same.

p. 11, l. 6-9: Redundant with p. 9, l. 9-11.

The reference to Bedmap2 on page 9 has been removed.

Response to Reviewer 2 (Xylar Asay-Davis)

General comments:

This paper presents a new method for computing basal melt rates below Antarctic ice shelves based on a polynomial best-fit to a non-dimensionalized 1D plume model. The major innovation of this work is the methods for computing the parameters (the slope of the ice draft and the height above the grounding line) for the 1D plume fit based on 2D ice and bedrock topography data. The result appears to be a low-cost, physically based method that can capture the large range of observed mean melt rates for groups of Antarctic ice shelves. Melt rate patterns are also argued to be closer to observations than those from other melt parameterizations, though this is not shown quantitatively.

This work represents a *significant* step forward in bridging the gap between more complete representations of sub-ice-shelf dynamics (e.g. in 3D ocean models or 2D plume models) and simplified, ad hoc melt parameterizations that contained little or no physics. Given the computational expense of ocean and plume modeling and the fact that ice-sheet models are not fully coupled into earth system models, there is a need in the ice-sheet modeling community for parameterizations and simplified models like the one proposed here to improve the realism of forcing from basal melting in response to changes in ocean temperature.

Thank you for this compliment. This is exactly the aim of our work and it is reassuring that this is acknowledged as a significant step.

The main concern I have with the paper involves the discussion around the temperature correction field ΔT applied to the observed temperatures from World Ocean Atlas (WOA). First, the claim is made that this correction is necessary because of unknown temperatures below the ice shelves, summer biases of observations and the interpolation method used to produce the base temperature field T_0 from WOA. No doubt, these factors do contribute to ΔT . But inaccuracies in the plume model itself are also being swept into ΔT . It is reassuring, as the authors state, that the ΔT is not unrealistically large (as they show it to be for an alternative parameterization), suggesting the strength of the plume-based parameterization. At the same time, the authors' sensitivity study in Sec. 3.1 shows that melt rates can be highly sensitive to changes in temperature that are of the same order as ΔT . This suggests that the evolution of melt rates, even if they are calibrated to match present-day observations, are likely to be highly sensitive to ΔT . This is not shown or discussed in the paper. An application of this parameterization in ice-sheet simulations forced by time-evolving ocean observations or simulation results would require a method for determining ΔT . The paper would benefit from some more discussion of how the authors foresee ΔT being computed in these scenarios. Namely, what ocean state should be used to compute ΔT ? Observations? The initial state of the ocean forcing? How sensitive are the melt rates likely to be to this choice?

The computation of the effective temperature field (more precisely ΔT) is indeed the main uncertainty in our study. We regret that it has led to so much confusion and agree that the method should be explained more clearly and its consequences discussed more critically. First of all, some changes were made to Sec. 3.2 that hopefully describe the method to calculate ΔT more clearly. Furthermore, a new Discussion section was added where we discuss various aspects of the model, including the calculation of ΔT and the temperature sensitivity. A proper temperature sensitivity study of the model is certainly a necessary step, preferably in combination with a dynamical ice sheet model and possibly also with ocean model results.

Another comment is that this paper relies heavily on Jenkins (2014), an EGU talk that does not seem to be available online. This work is cited 9 times, often with the implication that the reader should be familiar with the equations and notation it uses. I happen to have attended this particular EGU session but, as remarkable as the talk was, I can't say I remember the notation in detail. Given how heavily this work relies on Jenkins (2014), it might be worth either providing a permanent URL to that those slides or providing their contents as an appendix here. Otherwise, I would suggest efforts be made to cut down on how often that work is cited and instead to incorporate its findings directly into the paper.

As already mentioned to Reviewer #1, we fully agree that this is a weak point. The reason why we were rather concise in providing details from Jenkins (2014) is that a second paper is planned in which the derivation of the parametrization will be discussed in detail.

Instead of providing a permanent link to the slides, which probably would not completely solve the confusion and is also not free of objections, we have decided to restructure and rewrite Sec. 2.2., also after suggestions by Reviewer #1. Furthermore, we have added some recently found analytical arguments to Appendix A that further explain the form of the different factors in the parametrization.

The important thing to keep in mind is that the current parametrization is merely the result of an empirical study with the plume model. All notation and equations needed to run the model are fully described in the current manuscript. The revision of Sec. 2.2 and additional theoretical arguments in Appendix A further explain the background of the parametrization. Hopefully this clarifies where it all comes from without having to rely on the EGU talk. We hope to formalize the analysis in a future publication.

In addition to the requested discussion above, I recommend a number of minor revisions to the manuscript in the specific comments below. If these are addressed, I would recommend the manuscript for publication.

Specific comments:

In what follows, I will indicate the page number a line number as pp-ll (e.g. 1-1 for page 1, line 1) for simplicity.

2-9: “depend solely on the thickness of the water column beneath the ice shelf” I’m not aware of any parameterizations that use the thickness of the water column only, and the authors don’t give a citation for this. Instead, most parameterizations I’m aware of depend only on the depth of the ice-ocean interface (the ice draft), with some parameterizations (e.g. Asay-Davis et al. 2016) *also* using the water-column thickness to taper off melting near the grounding line.

We apologize for the confusion. This type of parametrization is present in our own ice model IMAU-ICE. It makes sense that such a parametrization is not really used in any publication, because it completely lacks a physical basis, giving the exact opposite behaviour from what we describe here (zero melt at the grounding line and monotonically increasing towards the ice front). It seems best to remove the references to such crude models from the manuscript. We have added a reference to the type of parametrization in your paper instead.

2-14: “Due to their steady nature, it is unlikely that the simple basal melt parameterizations contain enough physical details to capture this complex pattern without either significant tuning or extremely detailed ocean-shelf-cavity models.” First, I have trouble following what it meant by “their steady nature”. Do the authors mean their lack of dependence on external forcing (e.g. ocean temperature)? Or that they assume steady state? Or something else, perhaps? Second, “simple basal melt parameterizations” by definition will not be “extremely detailed ocean-shelf-cavity models”, so I think the sentence needs to be rephrased to differentiate between parameterizations and detailed physical models.

Thank you for this suggestion. We have changed this sentence in such a way that it refers more specifically to the local (steady was indeed not a good term) ice-ocean heat flux on which the “simple parametrizations” are based. Our point was that the local heat flux formulation could be used either by itself as a parametrization or as a boundary condition for a coupled ice-ocean model. But indeed, it is not correct to say that a simple parametrization is used with an extremely detailed physical model.

3-10: “Special attention is given to the construction of an effective ocean temperature field from observations, which is required for providing realistic input data of the temperature within the ice-shelf cavities to the parametrization.” This is part of my concern about how the ΔT field is discussed in this paper. I don’t disagree that there are biases in the the WOA observations but I do not think the authors demonstrate (or can demonstrate) that the correction leads to a more realistic temperature field. Instead, it is important to acknowledge that the various biases in the WOA observations, the interpolation/extrapolation of those observation, and the plume emulator are all being compensated by tuning ΔT , and this process will not necessarily mean that the resulting effective temperature is more realistic than WOA.

We fully agree with this view and have rephrased this particular sentence in the Introduction. As discussed below for Sec. 3.2, we have also added some more critical lines to the Discussion section.

4-3: "The non-linearity arose because the exchange velocity γ_T in Eq. (1a) was expressed as a linear function of the ocean current driving mixing across the boundary layer." This is not quite sufficient to have nonlinearity. It is also important that the strength of the ocean current is itself a function of the thermal driving. Maybe add something like, "...across the boundary layer, which is itself a function of the thermal driving".

This is indeed a necessary requirement. We have added some additional information, as also requested by Reviewer #1.

5-11, 5-12, 5-14: These are not the standard uses of the symbols Γ_T and Γ_S (e.g. Jenkins et al. 2010, Jenkins 2011). The exchange coefficients are typically defined to be distinct from the Stanton number, such that $St = (C_D)^{1/2} \Gamma_T$ (and similarly for salt). I would *strongly* recommend switching to this more standard notation or there is likely to be confusion when others try to implement the parameterization. (2c) and (2d) would therefore each need an extra factor of $(C_D)^{1/2}$ and this change would propagate to many other places in the manuscript.

Thanks for noting this discrepancy. We have corrected it throughout the manuscript.

6-12: "This simplified formulation can be used together with the prognostic equations (2) by assuming $T_b = T_f$ " My understanding of the 2-equation formulation is not that one necessarily assumes that $T_b = T_f$, but rather that a new equation is adopted with the same form as (2) with T_b substituted by T_f . We never need to know what T_b is but if one were to need it (e.g. as an ice-sheet boundary condition), it would be different from T_f because of the significantly lower salinity at the interface.

This is true. We have reformulated this.

6-15: "Also note the similarity between Eqs. (6) and the simple melt model described by Eqs. (1), the difference being the inclusion of heat conduction and the parametrization $\gamma_T = \Gamma_{TS} U$." I would say an equally (or perhaps more) important difference is the use of the plume T and S instead of the ambient fields.

This has been added.

6-19: "...different vertical temperature and salinity profiles of the ambient ocean (Jenkins, 2011, 2014)." My understanding is that the polynomial emulator that the authors use does not account for stratification or vertical variations in T and S. This might be worth mentioning explicitly, either here or better yet in the discussion section. Accounting for T and S profiles that vary with depth as well as time would be a potential improvement for the future that might allow the parameterization to produce Mode 3 seasonal melting (as defined in Jacobs et al.

1992) near the calving fronts of “cold” cavities. This could potentially improve the melt pattern.

We apologize if this was not clearly stated. The parametrization is indeed derived without taking into account vertical variations in T and S (as we now clarified in Sec. 2.2 and Appendix A). The original plume model does allow for vertical profiles. It also remains possible to use varying temperatures also in the parametrization, although this is not consistent with its derivation. We added a sentence at the start of Sec. 2.2 to clarify this and also refer to it in the new Discussion section.

7-9: “three larger length scales” If it is clear which 3 of the 4 length scales is largest, I missed it. It might be best to explicitly state either which 3 are meant or which one is excluded.

To be precise, Jenkins 2011 actually discusses all four length scales mentioned here. The crucial thing here is “beyond the initial zone near the grounding line where the initial source of buoyancy dominates”, implying that the third length scale mentioned here can be disregarded. To help the argument, we simply changed “three larger length scales” to “these length scales”, which hopefully avoids similar confusion.

7-17: “...the slope affects the entrainment rate, but not the melt rate...” I carefully read the corresponding section of Jenkins (2011) and I think what is shown is that the term in the mass conservation equation for the melt rate doesn’t explicitly contain the slope, whereas the term for the entrainment rate does. However, when the equations are solved, the resulting melt rate will depend on the slope, since the plume speed and thermal driving (which contribute to this the melt rate, as shown in Jenkins (2011), Eq. (14)) depend on the slope. So I think the phrase should be changed to something like “...the entrainment rate explicitly depends on the slope, whereas the melt rate does not...”

This is a good point. We have changed it accordingly.

9-9: “In this study, we use remapped data based on the Bedmap2 dataset for Antarctica (Fretwell et al., 2013),” Do the authors perform any kind of a firn correction to the ice thickness, given the assumption of constant ice density in the masking in Table 2? How well does the mask for grounded ice, floating ice and open ocean from Bedmap2 compare with that from the approach in Table 2? The figures suggest that the grounding line might not match well with Bedmap2 (e.g the Amery and deeper parts of the Ross and FRIS) but part of this could be due to the relatively coarse resolution. Without a firn correction, I wouldn’t expect the masking from Table 2 to be a good match to the mask provided with Bedmap2.

To our knowledge, no firn correction is adopted in the remapping procedure. This indeed causes a discrepancy between the current mask and the Bedmap2 mask. We think this might not cause big problems for the current coarse resolution (see also below), but it would be important to take into account if one

aims for very accurate simulations with high resolutions. Some words about this have been added to end of this section.

10-8: "the algorithm searches in this direction for the nearest ice-sheet point." This may be obvious to the authors but I think the method used to search for the nearest ice-sheet point should probably be stated explicitly. This part of the algorithm seems like it could potentially be quite slow, particularly at higher resolution. There might also be approaches (e.g. working out from the grounding line, caching the distance to the G.L. in each direction) that could be used to speed up the process. Is this something the authors have considered?

Some lines have been added that should further clarify the searching method. We admit that this is perhaps the simplest and one of the least efficient searching algorithms one could apply. But for the current resolution, the speed of the algorithm appears to be acceptable, also in the (preliminary) runs we have done with the parametrization coupled to our ice sheet model. But for high resolution it could indeed become much slower, and probably some revision of the algorithm would be needed. Some words on the efficiency have also been added to the Discussion section.

11-Fig. 3: "d n = 1/2(H b,1 + H b,2)" why the factor of 1/2 exactly here? Is this because the grounding line is assumed to always fall on the edge halfway between a grounded and a floating point? Also, the reasoning behind the different approaches in (b) and (c) probably deserves a bit more explanation.

This is indeed the assumption behind this additional interpolation. We have found that in some cases the depth difference between the first encountered ice-sheet point and the previous shelf point can be considerable. The additional interpolation is meant to smoothen these discrepancies. For higher resolutions, such an additional step might not be necessary. Also, there might be more sophisticated ways to estimate the location of the grounding line. Furthermore, the reason for having the two different approaches in (b) and (c) is simply to account for both positive and negative basal slopes behind the grounding line, assuming that the basal slope of the ice shelf is always positive. A brief discussion of this step has been added after the description of step 2 of the algorithm.

11-8: Why such coarse resolution (20 km)? Is the algorithm too costly to apply on finer resolution? Have the authors explored whether it still works at, say, 1 km resolution that seems to be needed to resolve grounding line dynamics? I could imagine that issues with noise due to rapid changes in bed slope (e.g. Fig 5b) would be exacerbated by finer resolution.

20 km is the resolution we are aiming for in our ice sheet model (IMAU-ICE). It seemed natural to use this resolution in the current study because we wish to calculate basal melt rates within the framework of future dynamic runs of the ice sheet model on a continental scale. As a crude test, we also applied the parametrization to the original 1 km resolution of Bedmap2. In that case, one resolves more detailed topographic features of the ice shelf base (channels) with

typically higher melt rates “following” these channels. But it is not clear if resolving such detailed features is realistic: they do not seem to appear in the Rignot map and we are also not resolving the 2D ocean circulation, which might be a more important effect. The current algorithm is nothing more than a description of a net circulation within the cavity. This is also mentioned in the Discussion section.

12-Fig. 4: There is a strange rim of floating ice around the whole of Antarctica not present in Bedmap2. Is that an artifact of the remapping scheme that was used? Or the masking scheme in Table 2? Perhaps the calving front is being smoothed out over multiple cells, leading to apparent floating ice where none was present in Bedmap2 before remapping? Also, as mentioned above, the grounded vs. floating mask doesn’t look like Bedmap2. Is this just the coarser resolution or has something gone wrong either during remapping or the masking procedure in Table 2?

The strange rim seems to be an artefact of Matlab’s `contourf` routine (i.e. the mask values are interpolated in order to determine the contour lines). We apologize for the confusion here. We changed Fig. 4a such that each pixel is plotted separately. The rim around the coastline has mostly disappeared, though there are still some isolated pixels here and there that are the direct result of our mask applied to the remapped Bedmap2 data. Note that we also changed the colours in the other panels of Fig. 4 as requested by Reviewer #1.

12-2: “The values for the local slope are typically higher both near the grounding line and the ice front, as shown in Fig. 4c.” Could the steeper slope the authors see near the ice front be an artifact of smoothing or remapping? The cross sections in Figs. 5a and 6a look quite smooth, even given the 20 km resolution, compared to plots of cross sections from Bedmap2 directly and I have not seen this tendency toward steeper slopes toward the calving front in sections I have taken from Bedmap2.

We have rephrased this sentence somewhat. It does seem true that higher slopes near the ice front are not very typical, neither in the original Bedmap2 data nor our generated slopes. But it does occur in a few places, notably FRIS, though maybe the slopes here are not as high as near the grounding line. Also, please note that Figs. 5 and 6 are not taken from Bedmap2, but from flow line data from Bombosch & Jenkins (1995) and Shabtaie & Bentley (1987).

13-20: “...the discrepancies between the current parametrization and the plume model are largest when the basal slope changes rapidly, because the parameterization responds immediately to the change while the full model has an inherent lag as the plume adjusts to the new conditions.” This problem will likely get worse at higher resolution. Might it be worth looking into a certain amount of along-flow smoothing and/or lag of when computing the effective α ? Perhaps something for the discussion section.

This is a good suggestion. We have added some lines to the Discussion section.

14-Fig 5, 15-Fig 6: It seems like what is potentially missing here is a comparison with the patterns from Rignot et al. (2013) or another melt rate field inferred from observations. I believe the Rignot data set is available from Jeremie Mouginot on request. The data set from Moholdt et al. (2014) is available from Gier Moholdt on request.

Thank you for this suggestion. We were able to obtain the data from Jeremie Mouginot, but we think it would be more appropriate to add a direct comparison to Sec. 3.3, because Fig. 5 and Fig. 6 are mainly meant to show the general 1-D behaviour of the plume model / parametrization. The full 2-D case including the algorithm of Sec. 2.3 is not yet discussed here. Please see our reply to your comment on Fig. 10 below.

15-4: "This also means that the simplest basal melt parametrizations currently used in some ice-sheet models, namely constant values or monotonic functions of the water-column thickness below the ice shelf, are far from being valid." Again, I don't know of any models using the latter. Perhaps the authors mean "ice draft" instead of "water-column thickness below the ice shelf"?

As mentioned earlier, these parametrizations occurring in our ice model are probably just for testing and not worth mentioning here, especially since they seem to lack a proper reference.

16-3: "but we will assume that the variations in ocean salinity around Antarctica are so small that the pressure freezing point T_f is only affected by variations in depth." What about buoyancy (via $\Delta\rho$)? Wouldn't this also depend on S_a ? Also, how has S_a been eliminated from the universal polynomial (given that it doesn't appear anywhere in Appendix A)? By assumption? Or has it been demonstrated in Jenkins (2014) that variations in S_a in the observed range don't have an appreciable effect? Would this still be true if stratification were taken into account?

The newly added analytical derivation in the Appendix should clarify how the buoyancy is actually parametrized in terms of $T_a - T_f$. We also refer to our reply to Reviewer #1's comment on the same line. What matters most is the salinity difference between the ambient ocean and the meltwater. This indeed depends directly on the absolute value of S_a , as well as indirectly through T_f , but the *horizontal* variations in S_a are assumed small. The factor Q_0 appearing in the Appendix is then approximately constant, and this constant essentially ends up in the parameter M_0 . Stratification would be an entirely different matter that is not captured by the current parametrization. We added some lines in this paragraph and in the new Discussion section that should cover this issue.

16-8: "The best possibility is an interpolated field..." First, I would rephrase "the best possibility" to something more like "We decide a more feasible approach was ...".

This phrase has been changed accordingly.

Second, to me it is odd to speak of interpolating the field into the ice-shelf cavities. It seems that this is what the authors did, but in my own modeling I extrapolate the field into a given cavity with no regard for temperatures in cavities on the other side of Antarctica that might figure into interpolation. Indeed, my colleagues and I have run into trouble when we were too naive in our extrapolation technique, extrapolating warm ocean temperatures from the Amundsen and Bellingshausen Seas under deep parts of FRIS. This does not appear to have occurred using the natural neighbors interpolation approach used here but it might still be worth acknowledging that interpolating temperature between ice-shelf cavities that really don't interact with one another is not really physically realistic.

We agree that one of the main drawbacks of a too simple interpolation technique is the occurrence of biases that are extrapolated from one cavity into another cavity, without taking into account that there might be a continent in between. We certainly encountered this problem as well and, as explained below, this was indeed one of the reasons for choosing the natural-neighbour approach, as it appears to minimize these effects. Still, these biases are still present and we should acknowledge this. Some sentences were added on page 18, which hopefully clarify this point ("One should note that both ... agree with the data of Rignot et al. (2013)").

16-16: "requires minimally tuned forcing data to produce realistic output." First, I'm not sure I agree with the assessment that the forcing in "minimally tuned", since the tuning likely has a significant effect on melt rates and their evolution, as discussed above. Second, I'm not sure I would characterize the computation of a field with 29 degrees of freedom (to match 13 mean melt rates) as "tuning", which in my experience refers to attempting to constrain a small number of model parameters rather than a spatially dependent field. Instead, this seems like inversion, much like the approach used to compute basal sliding factors under grounded ice in many ice sheet models. The authors have also characterized this as bias correction, but I do not necessarily agree with that characterization, as I stated above.

"Inversion" indeed seems to be a much better term. Thanks for this suggestion. We have tried to remove the phrases with "minimally tuned" and "realistic" and replace them with clearer and more objective terms.

18-2: "interpolated using natural-neighbour interpolation (i.e. a weighted version of nearest-neighbour interpolation, giving smoother results) to obtain data in the entire domain of interest." Again, it seems strange to interpolate *between* cavities. I guess natural-neighbor interpolation effectively extrapolate into cavities as long as the closest open ocean points is in front of *this* cavity and not some other cavity?

This is indeed what happens, at least if one would use *nearest*-neighbour interpolation. The weighting / smoothening in *natural*-neighbour interpolation probably causes temperatures from one cavity to "leak" into a separate cavity more easily. But this effect still seems much smaller than for e.g. linear

interpolation. We hope the added sentences (mentioned above) clarify that the interpolation method is still not perfect in this sense.

18-6: "this modification is necessary for eliminating biases in T_0 caused by the sparse observations and numerical interpolation, and also because the flow dynamics of the ocean are not resolved." This may be the principle but in reality the authors are almost certainly also correcting for shortcomings in the parameterization itself.

This is true and should be mentioned explicitly. We have chosen to add it to the Discussion section.

18-9: "29 carefully chosen points" I think more explanation is needed about how these points were chosen. It appears that they are located at grounding lines near the boundaries between shelves with potentially differing properties. Assuming ΔT is held fixed during an evolving simulation, will values of ΔT in regions that are currently grounded be appropriate as the grounding line moves? What might the limitations be? Again, this may belong in the discussion.

The 29 sample points have been chosen by a trial and error. We tried to clarify this in the text. One criterion is indeed to limit the biases near grounding lines resulting from the interpolation between ice shelves. But there are also regions (e.g. Dronning Maud Land) where warm open ocean temperatures are extrapolated into cavities due to the lack of cavity points in the observations. This causes higher values T_0 that would overestimate the melt rates (as we found) and require a negative ΔT .

Regarding the use of ΔT in evolving simulations, we realize that this is much less trivial than we might have anticipated. Some critical lines have been added in the Discussion section. A retreating grounding line is indeed one of the difficult issues here.

18-11: "Note that for technical reasons explained in Appendix A, we have applied a lower limit to the effective temperature equal to the pressure freezing point at surface level." As the authors show in the results section, this seems to be a significant limitation on the approach, particularly when applied to "cold" cavity shelves like FRIS. Perhaps some discussion is warranted on how this restriction might be relaxed in the future, as I will discuss more below.

It is certainly unsatisfying that this rather technical constraint still has a significant effect on the average melt rate for FRIS. We discuss this issue further below and in the Appendix. In the end, it seems to be just a consequence of the crudeness of the polynomial fit, rather than a physical constraint. The last sentence of the next paragraph, which claimed that the constraint has a physical meaning, has also been toned down.

18-18: The whole preceding paragraph for determining ΔT is the most worrisome aspect of the algorithm to me. The choice of ΔT (resulting from the details of how T_0 is computed) will potentially determine a lot about how melt rates evolve with time in response to changes in ocean temperature.

We have to admit that it is not entirely certain yet how this procedure should be translated to an evolving ocean, but some suggestions have been added to the Discussion section. With the current computation of T_{eff} we simply aim at obtaining a reasonable reference field that leads to the observed average melt rates. We hope that the critical notes added to the Discussion section address this issue.

18-28: "...yield realistic present-day melt rates for all shelf groups. Therefore, we can conclude that the effective temperature shown in Fig. 8b is a realistic forcing field, at least within the current modelling framework." I don't think the authors can make this statement. The field ΔT was inverted to yield realistic melt rates for the 13 ice-shelf groups, so the fact that this goal was reached does not suggest that the effective temperature is realistic. A comparison with observations not used to constrain the model would be needed to make such a conclusion. All the authors can conclude here is that their inversion worked as expected (except for FRIS) and that the resulting temperature field looks plausible.

True, this statement was too optimistic. We have removed it.

20-10: "This fact, along with the general melt pattern and the correlation with the surrounding ocean temperature, are in line with observations, e.g. Rignot et al. (2013)." This is by construction, so be careful not to attempt to use this as a validation of the model.

This is a good point. We have reformulated this sentence and also added a direct comparison with the Rignot data as suggested below.

20-11: "However, one should note that the Rignot et al. (2013) melt pattern shows a greater spatial variability, with more patches of (stronger) refreezing occurring between patches of positive melt. The lack of such prominent patches of refreezing in the current parametrization might have different reasons, such as the coarse resolution or the fact that we disregard the details of the ocean circulation within the ice-shelf cavities, as well as effects due to stratification and the Coriolis force." Lack of seasonal variability in T and S and also lack of vertical variability (not just in the sense of stratification, but also in the sense of having distinct water masses at different depths) likely also play a role. For example, this is likely why Mode 3 melting is missing (as mentioned above).

Thanks for this suggestion. We clarified it in the text.

20-15: "All in all, the plume parametrization, together with the effective temperature field, appears to give a realistic melt pattern for Antarctica, showing both a large spatial variability and average melt rates that agree with observations." It is definitely a strength of this parameterization compared with its predecessors that it can capture the range observed melt rates. So I definitely think this deserves emphasis. But, again, this is by construction. It is a good property to have but I think the authors should be careful to state that this is not

a validation of the model, since the observed melt rates were used in the inversion for ΔT .

We have removed this sentence here to make the description of the model results more objective. Also, a proper discussion of the parametrization seems to belong in the Discussion and Conclusion sections.

21-Fig 10: A comparison with the Rignot et al. (2013) melt rates seems like it would also make sense here. As I said, the data should be available on request. Having them plotted with the same color map would make them much easier to compare.

We have added a new figure (Fig. 12) with both the original Rignot dataset and the difference with the parametrization.

21-13: “minimal tuning” As before, I’m not a fan of this phrasing. What was done was an inversion of a field that can be argued to be within a plausible range. To me, this is neither clearly “minimal” nor clearly “tuning”.

This sentence has been rephrased.

23-1: “parametrizations based solely on the local balance of heat at the ice-ocean interface are not able to capture the complex melt pattern...” The authors can rightly claim to have a more broadly realistic melt pattern than these previous studies, with both melting and refreezing. But the authors have not really shown that the complex melt patterns resulting from their parameterization are contributing added realism compared to a simpler pattern with a similar distribution of melting and freezing, and complex patterns are not a goal in and of themselves.

It does not appear that we claim to have a fully realistic melt pattern in this particular sentence. Indeed, compared to the simpler models the new parametrization is more realistic because the simpler models cannot capture refreezing at all. We have tried to be more objective and critical throughout the manuscript, which hopefully solves this issue.

23-14: “...data from observations only need a minimal offset ΔT (between -1.4°C and 0.8°C)” Again, I would suggest a different phrasing than “minimal”. “Plausible”? Also, again I think some discussion is needed about how a time-varying T_0 field would be handled. Would ΔT be held fixed? (The authors seem to imply it would be)? How sensitive will the results likely be to ΔT ? Over what kinds of time scales might it be reasonable to hold ΔT fixed? How should data from ocean models be applied? Should a ΔT be computed from ocean-model initial conditions to match observed melt rates? Or should ocean observations (e.g. WOA) be used to compute ΔT ?

We have again removed the phrase “minimal” and changed it by “plausible”, which we find a better alternative. As mentioned above, the Discussion section now addresses the issue of using ΔT in the context of an ocean model.

23-22: "All in all, the presented plume parametrization, together with the constructed effective temperature field, gives realistic results for the present-day basal melt in Antarctica, both in terms of area-averaged values (Fig. 9) and the spatial pattern (Fig. 10a)." I don't think this paper as written has shown that the spatial patterns are realistic, just that the mean values are (by construction) consistent with observations. A more qualitative (or better yet quantitative) comparison of the spatial patterns with Rignot et al. (2013) or with another data set derived from observations would be needed to make the latter assertion here. Alternatively, the claim could be toned down, stating that the pattern is reasonable in a broad sense -- highest melt rates are near the grounding line with refreezing closer to calving fronts.

We think this is a good point, even though we have added the requested comparison of Rignot et al. (2013) in Fig. 12. There are still many features in the Rignot data that the current parametrization cannot capture. We have slightly rephrased this particular sentence.

23-29: "For such simulations, the effective temperature in Fig. 8b, even though it is a constructed field, can prove to be a valuable reference state to which temperature anomalies can be added." As I have said earlier, I think more discussion is needed on how the effective temperature would be used in dynamic ice-sheet simulations using this parameterization. This sentence is a good start but I'd really like to see more.

As mentioned already, this has been added to the Discussion section, with a reference to that section added here.

23-30 "Eventually, coupled ice-ocean simulations (e.g. DeConto and Pollard 2016) can benefit from this approach by comparing ocean-model output to this reference State." Hmm, I hope I'm misunderstanding but it seems like the authors are claiming that their reference temperature should act as a reference field, from which coupled ice sheet-ocean simulations could be validated. If this is not what was intended, please clarify what is meant here. If that is what is meant, that's a very bold assertion, given the fact that plume-model biases are also "swept under the rug" during the inversion process for ΔT used to produce the effective temperature field.

Sorry for the confusion, this is really not what we meant. As noted before, we fully agree that T_{eff} and ΔT contain model uncertainties as well and should be regarded as part of the model. In fact, ΔT also includes uncertainties in the observations used to constrain the melt rates. The idea would be to somehow use this information together with the ocean model output to obtain some reasonable evolving temperature anomaly that forces the melt rates. But as we tried to explain in the Discussion this is not completely clear yet, and of course validation of the coupled models is an entirely different matter altogether. We have tried to clarify this final sentence of the Conclusion section.

24-9, 24-11 The numerical constants 3.5e-5 and 10 seem to need units of m and m/yr/°C2, respectively. Maybe give them names and put them in a table or something, along with 0.545? Also, how were (A2) and (A3) derived, at least in broad strokes?

These parameters have been renamed and added to table 1. The (empirical) derivation of (A2) and (A3) is discussed in Sec. 2.2. We have added some clearer references to this section. Also, the newly added analytical derivation in this appendix should further clarify the background of these equations.

24-15: x 0 is unitless? How was it derived?

It is indeed unitless and determines the transition point between melting and freezing. Like the other parameters, it was derived empirically from the plume model results. We hope this has been clarified in the text.

24-22: Reading Jenkins (2011), it seems like $X > 1$ means there is no momentum left in the plume, so I would expect setting $m = 0$ beyond this point would be more realistic than restricting T_a to not go below the surface freezing point. By the way, it might be worth discussing why, physically, X should not be allowed to exceed 1.

This is indeed what happens physically. The suggestion to put $m = 0$ for $X > 1$ does seem to be a good alternative. We have added some words about this in the Appendix. However, the current melt curve (Fig. 2) does not exactly go to zero, so that putting $m = 0$ outside of the domain would lead to a discontinuity. Another alternative might be to just constrain X to lie between 0 and 1. All in all, this seems to be a rather technical problem pertaining to the crudeness of the polynomial fit. A proper analysis of the equations as we outlined at the end of the appendix might also lead to a “cleaner” formulation of the parametrization that overcomes this issue entirely.

25: It's not clear to me that Appendix B adds much to the text, other than to emphasize that the algorithms for finding z_{gl} and α are arbitrary. The results are visibly less realistic than for the algorithm presented in the main text and the problems with the constraint on T_a seem more severe. If you add Jenkins (2014) as an appendix, you might consider removing this one.

This appendix has been removed. Indeed, it seems better to focus on the current method and improve the description of the parametrization and the discussion of its limitations.

One final comment. Since your paper was submitted, an alternative method for parameterizing basal melt by Reese et al. (2017) has been submitted and is also on The Cryosphere Discussions (see full citation below). You might consider discussing how their approach compares with yours, including what the strengths and weaknesses of each approach might be for adoption in a full ice-sheet simulation. I don't mean this as shameless self promotion even though I'm a coauthor. I really do think these papers are highly relevant to one another.

Thank you for pointing our attention to this other paper. It is certainly interesting and useful to briefly discuss the differences and similarities between these two methods. Though it is difficult to fully grasp the behaviour of the PICO model just from reading the paper, it appears that both this model and our parametrization essentially describe the same physics: a net circulation within the cavity that requires an additional algorithm to be extended to 2-D. Judging from the reviewer comments of the other manuscript, both methods are also similar in terms of the physical processes that are not taken into account (e.g. stratification, Coriolis force etc.). If this is correct, then the main difference with our parametrization appears to be that it is a box model rather than based on a smooth fit function of the governing equations. It probably goes too far to add a detailed discussion of advantages and disadvantages of box models compared to parametrizations that are closer to the governing equations. In the end both are only approximations and both could give useful results. Of course, a lot depends also on the implementation and efficiency. Though one could argue that ultimately a systematically derived analytical solution/approximation of the plume equations might be preferred (we are not claiming that we have done this, but it would be an interesting next step). A few lines about this have been to the Discussion section.

Typographic and grammatical corrections:

1-1: It is a very minor thing but I would suggest another word or phrase besides “decline”, which implies to me that the AIS used to be better than it is now. Perhaps “...major factor in the decline in volume of the Antarctic Ice Sheet” or “...major factor in mass loss from the Antarctic Ice Sheet”. Also, “Ice Sheet” should be capitalized in this case.

corrected

2-13: “...a complex spatial pattern, which depends heavily on both the geometry below the ice shelves and the ocean temperature.” I do not think the observations demonstrate this, though I agree that it is the case. Perhaps rephrase something like “...a complex spatial pattern, which can be inferred to depend heavily on...”

corrected

2-17: “within a single ice-shelf cavity” Maybe consider “within individual ice-shelf cavities” instead, since we aren’t talking about one specific ice-shelf cavity but rather about any one of several ice-shelf cavities in isolation.

corrected

6-30: “The first governing length scale is associated with the pressure dependence of the freezing point that imposes an external control on the relationship between plume temperature, plume salinity and the melt rate, which is determined by the temperature relative to the freezing point.” I don’t

follow this sentence. What is determined by the temperature relative to the freezing point? Perhaps try to reword or break this sentence into 2.

The final clause has been removed because it indeed adds little clarification, especially since we have added more equations that explicitly show this relation.

10-17: "found values" should be "values found"

corrected

23-17: "The latter behavior is also apparent in..." It's not entirely clear to me what is meant by "the latter behavior". I guess it is the low sensitivity of the melt rate to changes in temperature, though this is not explicitly the behavior described in the previous sentence.

This sentence has been rephrased.

Modelling present-day basal melt rates for Antarctic ice shelves using a parametrization of buoyant meltwater plumes

Werner M. J. Lazeroms¹, Adrian Jenkins², G. Hilmar Gudmundsson², and Roderik S. W. van de Wal¹

¹Institute for Marine and Atmospheric Research Utrecht, Utrecht University, Utrecht, The Netherlands

²British Antarctic Survey, Natural Environment Research Council, Cambridge, United Kingdom

Correspondence to: Werner M. J. Lazeroms (w.m.j.lazeroms@uu.nl)

Abstract. Basal melting below ice shelves is a major factor in ~~the decline of the Antarctic ice sheet~~[mass loss from the Antarctic Ice Sheet](#), which can contribute significantly to possible future sea-level rise. Therefore, it is important to have an adequate description of the basal melt rates for use in ice-dynamical models. Most current ice models use rather simple parametrizations based on the local balance of heat between ice and ocean. In this work, however, we use a recently derived parametrization of the melt rates based on a buoyant meltwater plume travelling upward beneath an ice shelf. This plume parametrization combines a nonlinear ocean temperature sensitivity with an inherent geometry dependence, which is mainly described by the grounding-line depth z_{gl} and the local slope α of the ice-shelf base. For the first time, this type of parametrization is evaluated on a two-dimensional grid covering the entire Antarctic continent. In order to apply the essentially one-dimensional parametrization to realistic ice-shelf geometries, we present an algorithm that determines effective values for z_{gl} and α for any point beneath an ice shelf. Furthermore, since detailed knowledge of temperatures and ~~flow circulation~~[patterns in the ice-shelf cavities](#) is sparse or absent, we construct an effective ocean temperature field from observational data with the purpose of matching (area-averaged) melt rates from the model with observed present-day melt rates. The result is a [qualitatively](#) realistic map of basal melt rates around Antarctica, not only in terms of average values, but also in terms of the spatial pattern, with high melt rates typically occurring near the grounding line. The plume parametrization and the effective temperature field are therefore promising tools for future simulations of the Antarctic ~~ice sheet~~[Ice Sheet requiring a more realistic oceanic forcing](#).

1 Introduction

The Antarctic ~~ice sheet~~[Ice Sheet](#) is characterized by vast areas of floating ice at its margins, comprising ice shelves, both large and small, that buttress the outflow of ice from inland. The stability of these ice shelves is governed by a delicate mass balance, consisting of an influx of ice from the glaciers, iceberg calving at the ice front, snowfall and ablation at the surface, and basal melting due to ~~the flow of ocean water~~[oceanic heat exchange](#) in the ice-shelf cavities. Recent studies suggest that Antarctic ice shelves are experiencing rapid thinning (Pritchard et al., 2009, 2012; Paolo et al., 2015), an effect which can be traced back to an increase in basal melting (Depoorter et al., 2013; Rignot et al., 2013). This is especially apparent in West Antarctica, where relatively warm ocean water in the Amundsen and Bellinghausen seas is able to flow into the ice-shelf cavities and enhance melting from below. Increased basal melt rates and thinning of ice shelves decrease the buttressing effect, enhancing

the ice flow and associated mass loss from the Antarctic glaciers and ice sheet. ~~This~~ ~~The disintegration of the ice shelves~~ can significantly affect future sea-level rise, as suggested by recent numerical simulations (Golledge et al., 2015; Ritz et al., 2015; DeConto and Pollard, 2016).

~~In view of these issues~~ ~~In order to correctly predict the evolution of the ice sheet~~, it is necessary to have accurate models of the dynamics of ice shelves, in which basal melting at the interface between ice and ocean plays an important role. State-of-the-art ice-sheet models for large-scale climate simulations (see e.g. De Boer et al. 2015) provide a complete description of the flow and thermodynamics of ice. ~~Due~~ ~~However, due~~ to the complex nature of the system and high computational cost of climate simulations, these models inevitably contain approximations and parametrizations of many physical processes, among which basal melting is no exception. In particular, it is challenging to resolve the ocean dynamics within the ice-shelf cavities at a continental scale, which severely restricts the level of detail possible in basal melt parametrizations. ~~These parametrizations can be as simple as constant values or depend solely on the thickness of the water column beneath the ice shelf. However, most~~ ~~Most~~ recent simulations (e.g. De Boer et al. 2015; DeConto and Pollard 2016) determine the basal melt rate from ~~a steady state~~ ~~the local~~ heat flux at the ice-ocean interface (Beckmann and Goosse, 2003), driven by a far-field temperature and a number of tuning factors. ~~Others include a dependence on the thickness of the water column beneath the ice shelf in order to reduce melting near the grounding line (Asay-Davis et al., 2016).~~

As demonstrated by observational data (e.g. Rignot et al. 2013), the basal melt rates around Antarctica show a complex spatial pattern, which ~~depends~~ ~~can be inferred to depend~~ heavily on both the ~~geometry below the ice shelves~~ ~~geometry of the ice-shelf base~~ and the ocean temperature. ~~Due to their steady nature, it~~ ~~It~~ is unlikely that ~~the simple basal melt parametrizations contain enough physical details to~~ ~~a description of basal melt based on local fluxes at the ice-ocean interface can~~ capture this complex pattern without ~~either significant tuning or~~ ~~being either significantly tuned or used in conjunction with~~ extremely detailed ocean-shelf-cavity models. On the other hand, the ocean dynamics and associated melt rates within ~~a single individual~~ ~~ice-shelf cavity~~ ~~cavities~~ have been studied in rather high detail in recent years. For example, Holland et al. (2008) showed that basal melt rates obtained from a general ocean circulation model respond quadratically to changing ocean temperatures. These studies shed light on the minimal requirements of basal melt parametrizations, i.e. a nonlinear temperature sensitivity, an inherent geometry dependence corresponding to the unresolved ocean circulation, and a depth-dependent pressure freezing point, yielding higher melt rates at greater depths and the possibility of refreezing at lesser depths, ~~closer to the margins of the ice shelves~~.

~~Therefore~~ ~~Taking these requirements into account~~, we develop ~~here~~ a more advanced parametrization for the basal melt rates, based on the theory of buoyant meltwater plumes, which was first applied to the ice-shelf cavities by MacAyeal (1985). In this theory, it is assumed that the main physical mechanism driving the ocean circulation within the cavity is the positive buoyancy of meltwater, which travels upward beneath the ice-shelf base in the form of a turbulent plume. Melting at the ice-ocean interface is influenced by the fluxes of heat and meltwater through the ocean boundary layer, which depend on the plume dynamics. The upward motion of the plume induces an inflow of possibly warmer ocean water into the ice shelf cavity, creating more melt. Entrainment from the surrounding ocean water affects the momentum and thickness of the plume as it moves up

the ice-shelf base. Depending on the stratification of the ocean water inside the cavity, the plume may reach a level of neutral buoyancy from which it is no longer driven upward.

~~All these physical processes~~ The dynamics of the plume can be captured by a quasi-one-dimensional model of the mass, momentum, heat and salt fluxes within the plume~~and are~~, as shown schematically in Fig. 1. In particular, this work is based on 5 the plume model of Jenkins (1991), from which a basal melt parametrization has recently been derived (Jenkins, 2011, 2014). This parametrization is based on an empirical scaling of the plume model results in terms of ambient ocean properties and the geometry of the ice-shelf cavity. The geometry dependence is mainly determined by the grounding-line depth and the slope of the ice-shelf base. The aim of this particular study is to apply the plume parametrization to a two-dimensional grid covering 10 all of Antarctica, in order to investigate if this type of parametrization is able to give realistic present-day values and capture the complex pattern of basal melt rates shown in observations (Rignot et al., 2013).

In the following section, we describe the details of the plume model and the basal melt parametrization derived from it (Sections 2.1 and 2.2). An important part of the work is the development of an algorithm that translates the parametrization from a one-dimensional to a two-dimensional geometry, as described in Section 2.3. In Section 3.1, we show results from the numerical evaluation of the (still 1-D) parametrization along flow lines of two well-known Antarctic ice shelves, namely 15 Filchner-Ronne and Ross. Finally, Sections 3.2 and 3.3 discuss the application of the 2-D plume parametrization to the entire Antarctic continent, resulting in a two-dimensional map of basal melt rates under the ice shelves. Special attention is given to the construction of an effective ocean temperature field from observations, ~~which is required for providing realistic input data of the temperature within the ice-shelf cavities to the parametrization~~, by inversion of the modelled basal melt rates. The results are compared with those from simple heat-balance models (Beckmann and Goosse, 2003; DeConto and Pollard, 2016).

20 2 Modelling basal melt

In this section, we start with a description of the basic physics underlying basal melt models. We summarize the quasi-one-dimensional plume model of (Jenkins, 1991) and the development of the plume parametrization (Jenkins, 2011, 2014) resulting from this model. ~~In particular, we discuss the~~, as shown in previous work. The main contribution of the current study is 25 ~~the~~ method used to extend this plume parametrization to two-dimensional input data, necessary for use in a ~~fully functional ice-dynamical~~ 3-D ice-sheet–ice-shelf model.

First of all, we briefly discuss a common feature of many basal melt parametrizations, namely the dependence on the local balance of heat at the ice-ocean interface. In its simplest form, this is a balance between the latent heat of fusion and the heat flux through the sub-ice-shelf boundary layer, which can be expressed as follows (Holland and Jenkins, 1999; Beckmann and Goosse, 2003):

$$30 \quad \rho_i \dot{m} L = \rho_w c_w \gamma_T (T_a - T_f), \quad (1a)$$

where ρ_i, ρ_w are the densities of ice and ~~water~~ seawater, respectively, \dot{m} is the melt rate, L is the latent heat of fusion for ice, c_w is the specific heat capacity of ~~the ocean water~~ seawater, γ_T is a turbulent exchange velocity and T_a is the temperature of

the ambient ~~ocean water~~seawater. In this model, the melting is driven by the difference between T_a and the depth-dependent freezing point,

$$T_f = \lambda_1 S_w + \lambda_2 + \lambda_3 z_b, \quad (1b)$$

where S_w is salinity of the ~~surrounding ocean~~seawater, z_b is the depth of the ice-shelf base, and $\lambda_1, \lambda_2, \lambda_3$ are constant parameters. As explained by Holland and Jenkins (1999), more details can be included in this basal melt model, e.g. heat conduction into the ice and a balance equation for salinity (see also Section 2.1). Nevertheless, many ice models contain basal melt parametrizations based on Eqs. (1) (see e.g. De Boer et al. 2015; DeConto and Pollard 2016). These models typically use either constant or temperature dependent values for γ_T , leading to a melt rate that depends either linearly or quadratically on the temperature difference $T_a - T_f$. The latter case is consistent with the findings of Holland et al. (2008), who obtained a similar quadratic relationship from the output of an ocean general circulation model applied to the ice-shelf cavities. The non-linearity arose because the exchange velocity γ_T in Eq. (1a) was expressed as a linear function of the ocean current driving mixing across the boundary layer~~, which is itself a function of the thermal driving~~. Holland et al. (2008) further explain how this non-linear temperature dependence is related to the input of meltwater with an associated decrease in salinity and increase in buoyancy.

Hence, the exchange velocity plays an important role in correctly determining the heat balance at the ice-ocean interface, or, more precisely, the heat transfer through the ocean boundary layer beneath the ice shelves. However, a local heat-balance model as expressed by (1) is too simplistic to capture the effects of the ocean circulation on the basal melting, e.g. those depending on the ice-shelf geometry. The plume model and parametrization discussed in the remainder of this section are considered the next step in modelling the physics for general ice-shelf geometries without having to rely on full ocean circulation models, for which there are also insufficient input data to obtain a universal Antarctic solution.

20 2.1 Plume model

The parametrization used in this study is ~~ultimately~~ based on the plume model developed by Jenkins (1991). Here we summarize the key assumptions and physics behind this model. The ice-shelf cavity is modelled by a two-dimensional geometry (Fig. 1), in which the ice-shelf base has a (local) slope given by the angle α . This geometry is assumed to be uniform in the direction perpendicular to the plane and constant in time and can be seen as a vertical cross-section along a flow line of the ice shelf. We can define a coordinate X along the ice-shelf base with slope α and consider the development of a meltwater plume initiating at the grounding line ($X = 0$) and moving up along the ice-shelf base due to positive buoyancy with respect to the ambient ocean water.

The situation depicted in Fig. 1 essentially yields a two-layer system of the meltwater plume with varying thickness D , velocity U , temperature T and salinity S lying above the ambient ocean with temperature T_a and salinity S_a . As explained in Jenkins (1991), the typically small values of the slope angle α allow us to consider conservation of mass, momentum, heat and salt within the plume in a depth-averaged sense. Moreover, as the plume travels upward in the direction of X , it is affected by entrainment (at rate \dot{e}) of ambient ocean water, as well as the fluxes of meltwater (with melt rate \dot{m}) and heat at the ice-ocean interface (with temperature T_b and salinity S_b). These considerations yield the following quasi-one-dimensional system of

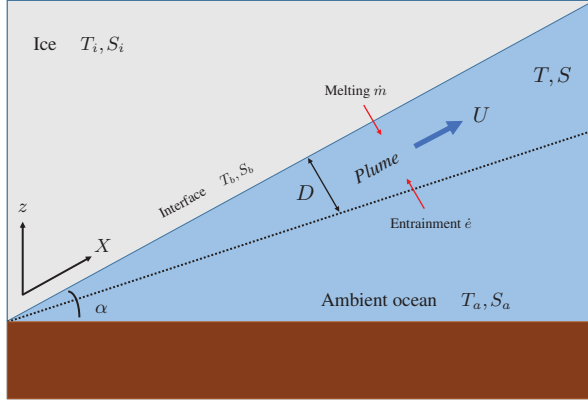


Figure 1. Schematic picture of the plume model. The plume travels upward under the ice-shelf base along the path X with speed U and thickness D while being influenced by melting and entrainment. Note that, in general, the slope angle α can vary in the direction of X .

equations for (D, U, T, S) as a function of the coordinate X along the shelf base, denoting the balance of mass, momentum, heat and salt within the plume:

$$\frac{dDU}{dX} = \dot{e} + \dot{m}, \quad (2a)$$

$$\frac{dDU^2}{dX} = D \frac{\Delta\rho}{\rho_0} g \sin \alpha - C_d U^2, \quad (2b)$$

$$5 \quad \frac{dDUT}{dX} = \dot{e} T_a + \dot{m} T_b - \underline{\underline{C_d^{1/2} \Gamma_T U (T - T_b)}}, \quad (2c)$$

$$\frac{dDUS}{dX} = \dot{e} S_a + \dot{m} S_b - \underline{\underline{C_d^{1/2} \Gamma_S U (S - S_b)}}, \quad (2d)$$

where g is the gravitational acceleration, C_d is the (constant) drag coefficient, $\Delta\rho = \rho_a - \rho$ is the difference in density between plume and ambient ocean, and $\underline{\underline{\Gamma_T, \Gamma_S, C_d^{1/2} \Gamma_T, C_d^{1/2} \Gamma_S}}$ are the turbulent exchange coefficients (Stanton numbers) of heat and salinity at the ice-ocean interface. The above formulation makes explicit the linear dependence of the turbulent exchange 10 velocities on the ocean current ($\underline{\underline{\gamma_T = \Gamma_T U, \gamma_S = \Gamma_S U}}$). The system of equations (2) is closed using suitable expressions for the entrainment rate \dot{e} , an equation of state $\rho = \rho(T, S)$, the balance of heat and salt at the ice-ocean interface and the liquidus condition. The expression for the entrainment rate is assumed to have the following form (Bo Pedersen, 1980):

$$\dot{e} = E_0 U \sin \alpha, \quad (3)$$

15 with E_0 a dimensionless constant. Hence, the entrainment rate increases linearly with the plume velocity, is zero for a horizontal ice-shelf base, and grows with increasing slope angle. Furthermore, a linearized equation of state yields:

$$\frac{\Delta\rho}{\rho_0} = \beta_S (S_a - S) - \beta_T (T_a - T), \quad (4)$$

where β_S is the haline contraction coefficient and β_T the thermal expansion coefficient. The boundary conditions at the ice-ocean interface are given by:

$$\underline{C_d^{1/2}} \Gamma_T U (T - T_b) = \dot{m} \left(\frac{L}{c_w} + \frac{c_i}{c_w} (T_b - T_i) \right), \quad (5a)$$

$$\underline{C_d^{1/2}} \Gamma_S U (S - S_b) = \dot{m} (S_b - S_i), \quad (5b)$$

$$5 \quad T_b = \lambda_1 S_b + \lambda_2 + \lambda_3 z_b \quad (5c)$$

i.e. the first equation balances the turbulent exchange of heat with heat conduction and latent heat of fusion L in the ice, where c_w and c_i are the specific heat capacities of seawater and ice, respectively, and T_i is the ice temperature. Similarly, Eq. (5b) is a balance between turbulent exchange of salt and diffusion into the ice. Eq. (5c) is the (linearized) liquidus condition that puts the interface temperature equal to the pressure freezing point at the local depth z_b of the ice-shelf base, ~~similar equivalent~~ to Eq. (1b).

Equations (2)-(5) form a closed set that can be solved to obtain the prognostic variables (D, U, T, S) of the plume as a function of the plume path X , given the ice-shelf draft $z_b(X)$ with slope angle $\alpha(X)$, the ambient ocean properties $T_a(z)$ and $S_a(z)$, and the ice properties T_i and S_i . Of particular interest for the current work, however, are the ice-ocean interface conditions (5), which essentially determine the melt rate \dot{m} , the key quantity of this study. In other words, the melt rate is determined by the fluxes of heat and salt at the interface, which in turn are linked to the development of the plume. Note that these boundary conditions can be simplified (McPhee, 1992; McPhee et al., 1999) to only two equations containing the freezing temperature T_f of the plume, rather than the interface properties T_b and S_b :

$$\underline{C_d^{1/2}} \Gamma_{TS} U (T - T_f) = \dot{m} \left(\frac{L}{c_w} + \frac{c_i}{c_w} (T_f - T_i) \right), \quad (6a)$$

$$T_f = \lambda_1 S + \lambda_2 + \lambda_3 z_b, \quad (6b)$$

20 where ~~$\Gamma_T \Gamma_S C_d^{1/2} \Gamma_{TS}$~~ is an effective heat exchange coefficient. This simplified formulation can be used together with the prognostic equations (2) ~~by assuming $T_b = T_f$, by substituting T_b with T_f in (2c) (note that T_b and T_f are not necessarily equal)~~, whereas S_b disappears from the problem by substituting (5b) in (2d). ~~As shown~~ Strictly speaking, Eq. (6) is only valid after assuming a constant ratio Γ_T / Γ_S of the exchange coefficients, as explained by Jenkins et al. (2010), ~~who also show that~~ both Eqs. (5) and Eqs. (6) give similar results when used to describe basal melt rates under Ronne Ice Shelf. Also note the similarity between Eqs. (6) and the simple melt model described by Eqs. (1), the difference being the inclusion of heat conduction and the parametrization ~~$\gamma_T = \Gamma_{TS} U, \gamma_T = C_d^{1/2} \Gamma_{TS} U$~~ as well as the plume variables T and S instead of ambient ocean properties. Hence, the turbulent exchange in this model is directly determined by the plume velocity that appears as a prognostic variable.

Without giving further details, we mention that the plume model described above can be evaluated for different ice-shelf geometries (i.e. vertical cross-sections along flow lines) and different vertical temperature and salinity profiles of the ambient ocean (Jenkins, 2011, 2014). In this model, the general physical mechanism governing the development of the plume is the

addition of meltwater at the ice-ocean interface, which increases its buoyancy. Changes in buoyancy affect plume speed and that, combined with its temperature and salinity, determines the subsequent input of meltwater.

2.2 Basal melt parametrization along a flow line

Evaluating the aforementioned plume model for different geometries and ocean properties leads to a wide variety of solutions for the basal melt rates. The question arises whether there exists an appropriate scaling with external parameters that combines these results into a universal melt pattern. Here we will summarize how such a scaling can be found, leading to the basal melt parametrization of Jenkins (2014) for the quasi-one-dimensional geometries along flow lines described in the previous section. [Section](#); more details can be found in [Appendix A](#). It is important to note that the following derivation is based on simple geometries with a constant basal slope and constant ambient ocean properties, though the resulting parametrization can easily be applied to more general cases, as shown in [Section 3.1](#). [Section 2.3](#) will discuss the extension of this parametrization to more realistic two-dimensional geometries.

The basal melt parametrization used in this study consists of a general expression for a dimensionless melt rate \hat{M} as a function of the dimensionless coordinate \hat{X} measured from the grounding line ([Fig. 2](#)). This dimensionless coordinate is essentially the vertical distance of the ice-shelf base from the grounding line, scaled by a temperature- and geometry-dependent length scale:

$$\hat{X} = \frac{z_b - z_{gl}}{l}, \quad l = f(\alpha) \cdot \frac{T_a - T_f(S_a, z_{gl})}{\lambda_3}, \quad (7)$$

where z_{gl} is the grounding-line depth and $f(\alpha)$ a slope-dependent factor. Hence, $\hat{X} = 0$ corresponds to the grounding line and any shelf point downstream from the grounding line corresponds to a value $0 < \hat{X} < 1$ depending on T_a , S_a , z_{gl} and α . This scaling also implies that the edge of the ice shelf is not necessarily located at $\hat{X} = 1$, but its location is highly dependent on the input variables. Similarly, the melt rate is scaled as follows:

$$\hat{M} = \frac{\dot{m}}{M}, \quad M = M_0 \cdot g(\alpha) \cdot [T_a - T_f(S_a, z_{gl})]^2 \quad (8)$$

with a different slope-dependent factor $g(\alpha)$ and a constant parameter M_0 . The dimensionless curve $\hat{M}(\hat{X})$ in [Fig. 2](#) is now defined by polynomial coefficients that were found empirically from the plume model results (Jenkins 2014; [Appendix A](#)). In summary, to obtain the basal melt rate \dot{m} at any point beneath the ice-shelf, one requires the local depth z_b , local slope α , grounding-line depth z_{gl} and ambient ocean properties T_a and S_a to calculate \hat{X} and find the corresponding value on the dimensionless curve $\hat{M}(\hat{X})$, which then has to be multiplied by the physical scale given in (8) (see [Appendix A](#) for details). The physical quantities and constant parameters required for evaluating the parametrization are summarized in [Table 1](#).

Although the scaling defined by (9) and (8) is found in a purely empirical way, it is possible to derive the various factors analytically, as sketched in [Appendix A](#). The empirical procedure and the physical meaning of the different factors are outlined in the following. A general solution to the problem is challenging to find as there are at least four length scales that determine the plume evolution (Jenkins, 2011). The first governing length scale is associated with the pressure dependence of the freezing

point that imposes an external control on the relationship between plume temperature, plume salinity and the melt rate, ~~which is determined by the temperature relative to the freezing point~~. Lane-Serff (1995) discussed how this length scale $(T_a - T_f)/\lambda_3$ ~~approximately~~ determines the distribution of melting and freezing beneath an ice shelf. Jenkins (2014) extended the analysis of Lane-Serff (1995) by making the transition point between melting and freezing dependent on the ice-shelf basal slope, resulting in the length scale (9) with slope factor $f(\alpha)$.

The second length scale is associated with the ambient stratification, which determines how far the plume can rise before reaching a level of neutral buoyancy. Magorrian and Wells (2016) discuss the plume behaviour and resulting melt rates when this length scale dominates. Critically, with the pressure dependence of the freezing point assumed to be negligible, as required in the analysis of Magorrian and Wells (2016), no freezing can occur. A third length scale can be formulated by comparing the input of buoyancy from freshwater outflow at the grounding line with the input of buoyancy by melting at the ice-ocean interface (Jenkins, 2011). This length scale indicates the size of the zone next to the grounding line where the impact of ice shelf melting on plume buoyancy can be ignored and conventional plume theory (Morton et al., 1956; Ellison and Turner, 1959) applied, and is generally small compared with typical ice shelf dimensions. A final length scale is that at which the Coriolis force takes over from friction as the primary force balancing the plume buoyancy in the momentum budget. Jenkins (2011) discussed ~~the three larger length scales~~ ~~these length scales~~ in the context of which would take over as the dominant control on plume behaviour beyond the initial zone near the grounding line where the initial source of buoyancy dominates, and showed the length scale associated with the pressure dependence of the freezing point (Eq. (9)) to be most important for typical ice-shelf conditions. ~~Hence, in order to obtain a universal curve for the melt rate beneath an ice shelf, Jenkins (2014) extended the analysis of Lane-Serff (1995), who showed how the length scale defined by:~~

$$20 \quad L = \frac{T_a - T_f}{\lambda_3}$$

~~approximately determined the zones of melting and freezing produced by the plume. The variation in the transition point from melting to freezing is a function of the ice shelf basal slope. As~~

The universal length scale l in (9) contains two more ingredients. First, ~~as~~ discussed by Jenkins (2011), the ~~slope affects the entrainment rate, but not~~ entrainment rate in the mass conservation equation (2a) explicitly depends on the slope α , whereas the melt rate ~~is only affected indirectly~~, so there is a geometrical factor that scales the elevation of the plume temperature above the local freezing point:

$$\frac{E_0 \sin \alpha}{\Gamma_{TS} + E_0 \sin \alpha} \frac{E_0 \sin \alpha}{C_d^{1/2} \Gamma_{TS} + E_0 \sin \alpha}. \quad (9)$$

~~Using this factor, a universal length scale can be empirically derived. This factor gives rise to the slope dependence $f(\alpha)$ in l , which is essentially an empirically derived scaling of the transition point between melting and freezing (Appendix A). Note that Jenkins (2011) simplified the plume model by using The second ingredient is related to the coefficient Γ_{TS} , which appears in $f(\alpha)$ through the simplified interface conditions (6) directly, whereas Jenkins (2014) retained the more complex melt formulation (5) in the plume model while seeking empirical scalings based on an effective Γ_{TS} . As discussed by Holland and Jenkins~~

(1999), the factor relating Γ_T and Γ_{TS} is itself a function of the plume temperature, so Jenkins (2014) expressed the effective Γ_{TS} as an empirical function of Γ_T , $T_a - T_f$ and (9) (see Appendix A). When distance along the plume path is scaled with this slightly more complex factor (see Eq. (A10)), the melt rates produced by the plume model conform to a universal form, first rising to a peak at the same scaled distance, before falling and transitioning to freezing at a common point ~~-(Fig. 2)~~.

5 With the distance along the plume path appropriately scaled, all that remains is to scale the amplitude of ~~the curves, the melt rate curves produced by the plume model and find the melt rate scale M in~~ (8). As in Jenkins (2011) the appropriate physical scales are: 1) the temperature of the ambient seawater relative to the freezing point; 2) the factor in Eq. (9) scaling the temperature elevation of the plume above freezing; 3) a factor that scales the plume speed, given by the ratio of plume buoyancy to frictional drag:

$$10 \quad \left(\frac{\sin \alpha}{C_d + E_0 \sin \alpha} \right) \left(\frac{\Gamma_{TS}}{\Gamma_{TS} + E_0 \sin \alpha} \frac{C_d^{1/2} \Gamma_{TS}}{C_d^{1/2} \Gamma_{TS} + E_0 \sin \alpha} \right). \quad (10)$$

The second term in parenthesis is the factor that scales the plume temperature relative to the ambient temperature and thus controls plume buoyancy. It replaces the initial buoyancy flux at the grounding line used in the scaling of Jenkins (2011). The final expression includes factors and powers that are derived empirically ~~to yield (though some theoretical arguments can be applied, cf. Appendix A), giving rise to the form of M with slope factor $g(\alpha)$ in~~ (8). The result of this scaling procedure is an approximately universal melt rate curve, which can then be represented by a single polynomial expression that is accurate to about 20% for melt rates ranging over many orders of magnitude (Jenkins, 2014).

15 ~~In application, the basal melt parametrization thus consists of a general expression for the dimensionless melt rate \hat{M} as a function of the dimensionless coordinate \hat{X} measured from the grounding line (Fig. 2). This dimensionless coordinate is essentially the depth difference $z_b - z_{gl}$ scaled by a temperature and depth dependent length scale. Hence, $\hat{X} = 0$ corresponds to the grounding line and any shelf point downstream from the grounding line corresponds to a value $0 < \hat{X} < 1$ depending on T_a and α . This scaling also implies that the edge of the ice shelf is not necessarily located at $\hat{X} = 1$, but its location is highly dependent on the input variables. In summary, to obtain the basal melt rate m at any point beneath the ice shelf, one requires the local depth z_b , local slope α , grounding line depth z_{gl} and ambient ocean properties T_a and S_a to determine the corresponding value on the dimensionless curve $\hat{M}(\hat{X})$, which then has to be multiplied by the physical scales given in Appendix A. The physical quantities and constant parameters required for evaluating the parametrization are summarized in Table 1.~~

2.3 Basal melt parametrization in 2-D: effective plume path

As explained in the previous section, an important feature of the basal melt parametrization is its dependence on non-local quantities, in particular the grounding-line depth z_{gl} from which the plume originated. Therefore, in order to apply the parametrization to realistic geometries, one needs to know for each ice-shelf point the corresponding grounding-line point(s) serving as the 30 origin of the plume(s) reaching that particular shelf point. For the quasi-one-dimensional settings considered so far, this is not an issue, since the plume can only travel in one direction. However, for general ice-shelf cavities, an arbitrary shelf point can be reached by plumes from multiple directions, corresponding not only to different values for z_{gl} , but also to different slope

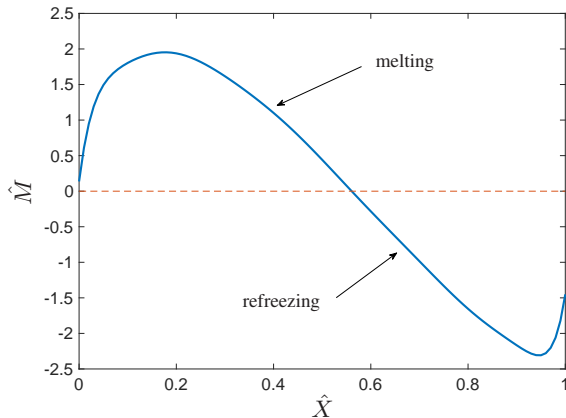


Figure 2. Dimensionless melt curve $\hat{M}(\hat{X})$ used in the basal melt parametrization. Higher melt rates typically occur close to the grounding line with a maximum at $\hat{X} \approx 0.2$. A transition from melting to refreezing may occur further away from the grounding line, depending on the position of the ice front. Note that the value of \hat{X} depends on the distance to the grounding line, as well as the temperature difference $T_a - T_f$ and the local slope α (see Appendix A). In other words, $\hat{X} = 0$ corresponds to the grounding line, but the dimensionless position of the ice-shelf front depends on the length scale and is not necessarily equal to $\hat{X} = 1$.

angles α . This means that the plume parametrization cannot be directly applied to such geometries. An algorithm is needed to determine effective values for z_{gl} and α , ~~which is discussed below. Note that~~ The development of this algorithm is ~~not unique; an alternative method with slightly different results is discussed in Appendix ??~~ the main focus of the current work and discussed below.

5 As a starting point, we consider the usual topographic data in terms of two-dimensional fields for the ice thickness H_i , bedrock elevation H_b and surface elevation H_s used by ice-dynamical models. ~~In this study, we use remapped data based on the Bedmap2 dataset for Antarctica (Fretwell et al., 2013), but the~~ The following algorithm is valid for any topographic data on a rectangular grid with any resolution $\Delta x \times \Delta y$. First of all, the topographic data are used to define an ice mask based on the criterion for floating uniform ice, as shown in Table 2. Furthermore, the depth of the ice base is ~~easily~~ determined to be:

10 $z_b = H_s - H_i.$ (11)

Now, in In order to apply the basal melt parametrization to this two-dimensional data, ~~we must determine~~ must be determined effective values for z_{gl} and α for every ice-shelf point (i, j) with basal depth $z_b(i, j)$, where the indices i and j denote the position on the grid. This is done by first searching for “valid” grounding-line points in 16 directions on the grid, starting from any shelf point (i, j) , as depicted in Fig. 3a. Note that we can calculate a local basal slope $s_n(i, j)$ at the point (i, j) in the n -th direction as follows:

$$s_n(i, j) = \frac{z_b(i, j) - z_b(i + i_n, j + j_n)}{\sqrt{(i_n \Delta x)^2 + (j_n \Delta y)^2}}, \quad (12)$$

Table 1. Physical quantities and constant parameters serving as input for the basal melt parametrization.

External quantities		Units
z_b	Local depth of ice-shelf base	m
α	Local slope angle	—
z_{gl}	Depth of grounding line	m
T_a	Ambient ocean temperature	°C
S_a	Ambient ocean salinity	psu
Constant parameters		Values
E_0	Entrainment coefficient	3.6×10^{-2}
C_d	Drag coefficient	2.5×10^{-3}
Γ_T	Turbulent heat exchange coefficient	1.1×10^{-5}
Γ_{TS0}	Effective heat exchange coefficient	6.0×10^{-4}
λ_1	Freezing point-salinity coefficient	-5.73×10^{-2} °C
λ_2	Freezing point offset	8.32×10^{-2} °C
λ_3	Freezing point-depth coefficient	7.61×10^{-4} K m $^{-1}$
M_0	Melt rate parameter	$10 \text{ m yr}^{-1} \text{ °C}^{-2}$
γ_1	Heat exchange parameter	0.545
γ_2	Heat exchange parameter	3.5×10^{-5} m $^{-1}$

where (i_n, j_n) denotes a direction vector on the grid, i.e. $(i_n, j_n) = (1, 0)$ denotes right, $(i_n, j_n) = (0, 1)$ denotes up, etc., and Δx and Δy denote the horizontal grid size in the x - and y -direction, respectively. To determine whether a grounding-line point found in one of the 16 directions is valid for the calculation of the basal melt, we apply the following two criteria are applied:

1. Assuming that a buoyant meltwater plume can only reach the point (i, j) from the n -th direction if the basal slope in that direction is positive, we only search the algorithm only searches in directions for which $s_n(i, j) > 0$.

2. If the first criterion is met for the n -th direction, the algorithm searches in this direction for the nearest ice-sheet point.

This point More precisely, the associated direction vector (i_n, j_n) is added to the grid indices and the mask value in the resulting point is checked. This process is repeated until either an ice-sheet point, an ocean point or the domain boundary is encountered. An ice-sheet point found in this way is only considered to be a valid grounding-line point if it lies deeper than the original ice-shelf point at (i, j) , assuming again that a buoyant meltwater plume from the grounding line can only go up. The second criterion then becomes $d_n(i, j) < z_b(i, j)$.

Note, however, that we can in determining the second criterion, the depth-difference between the encountered sheet point and the adjacent shelf point can be considerable, especially for coarser resolutions. In such cases, the algorithm tries to obtain a better estimate of the true grounding-line depth in this direction, say $d_n(i, j)$, if we interpolate by interpolating along either the

Table 2. Definition of the ice mask. The ice-shelf criterion is that for uniform ice with density ρ_i floating on ocean water with density ρ_w . The minimum ice thickness used here is $H_{i,\min} = 2$ m.

Mask value	Type	Criterion
0	ice sheet	$(\rho_i/\rho_w)H_i > -H_b$
1	ice shelf	$(\rho_i/\rho_w)H_i \leq -H_b$
2	ocean / no ice	$H_i \leq H_{i,\min}$

bed or the ice base, as shown in Fig. 3b and c. The ~~second criterion then becomes $d_n(i,j) < z_b(i,j)$.~~ ~~two cases shown in these figures account for either a positive or a negative basal slope beyond the grounding line. One should note that this additional step assumes the grounding line to be located halfway between the sheet and shelf points, which could be improved by more sophisticated interpolation techniques.~~

5 Following the above procedure yields for each ice-shelf point (i,j) a set of grounding-line depths d_n and local slopes s_n in the directions that are “valid” according to the aforementioned two criteria. Mind that not all directions may yield a (valid) grounding-line point, in particular those towards the open ocean. Now, in order to determine the *effective grounding-line depth* $z_{gl}(i,j)$ and *effective slope angle* $\alpha(i,j)$ necessary for calculating the basal melt in the shelf point (i,j) , we simply take the average of the ~~found values~~ ~~values found~~ for d_n and s_n :

$$10 \quad z_{gl}(i,j) = \frac{1}{N_{ij}} \sum_{\text{valid } n} d_n(i,j), \quad (13a)$$

$$\tan[\alpha(i,j)] = \frac{1}{N_{ij}} \sum_{\text{valid } n} s_n(i,j), \quad (13b)$$

where N_{ij} denotes the number of valid directions found for the shelf point (i,j) . On the other hand, if no valid values for d_n and s_n are found for a particular shelf point, we take $z_{gl} = z_b$ and $\alpha = 0$, leading to zero basal melt in that point (see Appendix A).

15 In summary, the method described above yields two-dimensional fields for the effective grounding-line depth z_{gl} and effective slope $\tan(\alpha)$, given topographic data in terms of H_i , H_s and H_b and a suitable ice mask, such as the one defined in Table 2. These fields, in turn, serve as input for the basal melt parametrization described in the previous section, together with appropriate data for the ocean temperature T_a and salinity S_a (discussed in Section 3.2). We thus obtain a complete method for calculating the basal melt for all Antarctic ice shelves, given the topography and ocean properties, which can also be used 20 in conjunction with ice-dynamical models. In the following, however, we use the Bedmap2 dataset (Fretwell et al., 2013) to define the present-day topography of Antarctica and disregard the ice dynamics. More specifically, the original Bedmap2 data is remapped to a rectangular grid with grid size $\Delta x = \Delta y = 20$ km, using the mapping package OBLIMAP 2.0 (Reerink et al., 2016). The resulting topographic data can be used as input for the algorithm described here, leading to the fields for z_{gl} and $\tan(\alpha)$ shown in Fig. 4, which are used for the basal melt calculations discussed in Section 3. ~~Note that the mask in Fig. 4a~~ 25 ~~does not exactly match the Bedmap2 mask because a constant ρ_i was used in formulation of Table 2 as is common in many~~

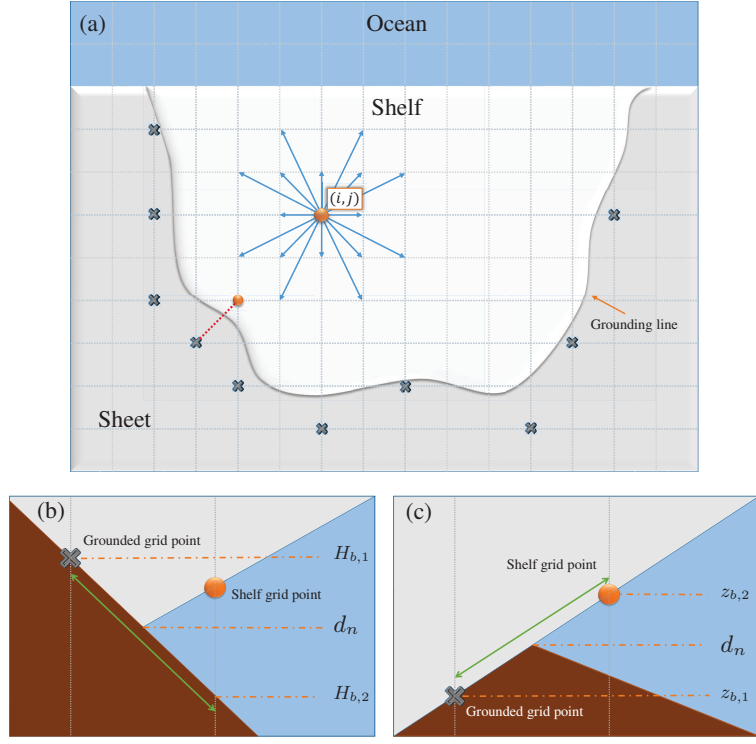


Figure 3. Schematic of the algorithm for finding the average grounding-line depth and associated slope angle used by the basal melt parametrization. (a) Top view of an ice-shelf on a horizontal grid. The algorithm searches in 16 directions on the grid from the shelf point (i, j) . Possible grounded points found in this way are marked by \times . (b) Vertical slice along the n -th direction (e.g. the red dotted line in (a)). If the grounded point is higher than the previous shelf point, the grounding-line depth d_n is found by interpolation along the bed ($d_n = \frac{1}{2}(H_{b,1} + H_{b,2})$). (c) Interpolation along the ice base if the grounded point in the n -th direction is deeper than the previous shelf point ($d_n = \frac{1}{2}(z_{b,1} + z_{b,2})$).

ice sheet models. This might cause discrepancies in the position of the grounding line, which, however, are likely compensated by the rather coarse resolution. In Fig. 4b one can see that the lowest values of z_{gl} are obtained towards the inland regions of Filchner-Ronne ice shelf and Amery ice shelf. The values for the local slope are typically higher both typically high near the grounding line and in some places also near the ice front, as shown in Fig. 4c.

5 One should note that, although we attempt to directly translate the concept of a quasi-1-D plume to a multitude of plumes in two dimensions, there are important physical effects not taken into account by this approach. Most importantly, a realistic two-dimensional plume has an additional degree of freedom because it also develops in the cross-flow direction, causing the width to be a dynamic variable in addition to the thickness D . This can have significant consequences for the mass budget currently described by (2a). Hattermann (2012) explored the possibility of adding a variable plume width to the original plume model and showed that such a 2-D formulation improves the prediction of melt rates for a realistic ice-shelf geometry compared

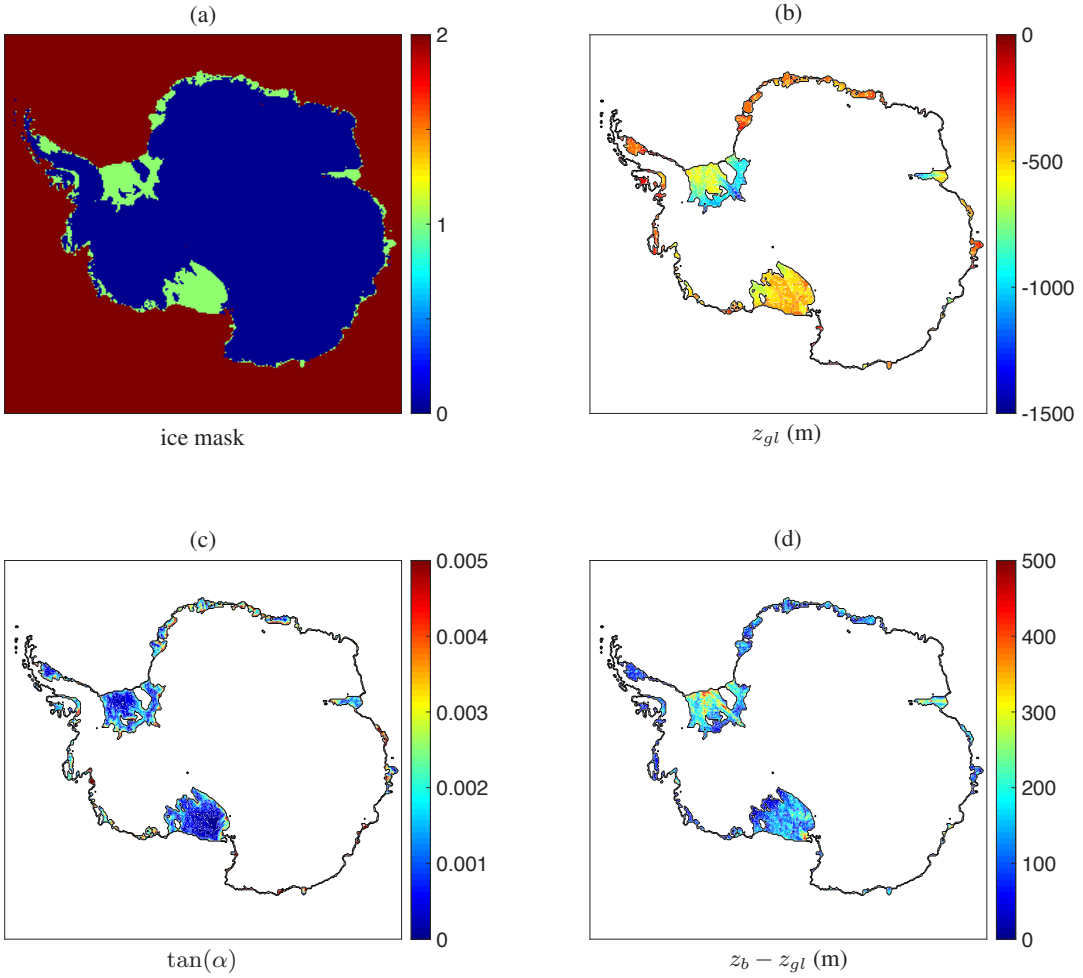


Figure 4. Effective plume paths under the Antarctic ice shelves as calculated by the algorithm of Section 2.3 using the Bedmap2 topographic data remapped on a 20 km by 20 km grid. (a) Ice mask according to Table 2. (b) The effective grounding-line depth z_{gl} . (c) The effective slope $\tan(\alpha)$. (d) The difference between local ice-base depth and associated grounding-line depth, $z_b - z_{gl}$.

to the 1-D model (Hattermann et al., 2014). Although this appears to be an important extension of the plume model that should be taken into account, the aim of the current work is to explore the capabilities of the original 1-D plume parametrization in predicting melt rates around Antarctica. The current approach is meant to be a simple method to parametrize the net circulation within an ice-shelf cavity as the average effect of multiple plumes, in order to be applied around the entire ice sheet. Further extensions for obtaining a 2-D plume model are beyond the scope of this work.

Table 3. Additional model parameters used for evaluating the plume model and the simple parametrizations described in Section 3.1.

Constant parameters		Values
L	Latent heat of fusion for ice	$3.35 \times 10^5 \text{ J kg}^{-1}$
c_w	Specific heat capacity of water	$3.974 \times 10^3 \text{ J kg}^{-1} \text{ K}^{-1}$
c_i	Specific heat capacity of ice	$2.009 \times 10^3 \text{ J kg}^{-1} \text{ K}^{-1}$
β_S	Haline contraction coefficient	7.86×10^{-4}
β_T	Thermal expansion coefficient	$3.87 \times 10^{-5} \text{ K}^{-1}$
g	Gravitational acceleration	9.81 m s^{-2}
ρ_i	Density of ice	$9.1 \times 10^2 \text{ kg m}^{-3}$
ρ_w	Density of ocean water	$1.028 \times 10^3 \text{ kg m}^{-3}$
γ_T	Turbulent exchange velocity (BG2003)	$5.0 \times 10^{-7} \text{ m s}^{-1}$
κ_T	Turbulent exchange coefficient (DCP2016)	$5.0 \times 10^{-7} \text{ m s}^{-1} \text{ K}^{-1}$

3 Results

Here we present various results obtained by evaluating the basal melt parametrization described in the previous section. First, we investigate the main characteristics of the original 1-D parametrization of Section 2.2 by evaluating it along flow lines of the Filchner-Ronne and Ross ice shelves. In Sections 3.2 and 3.3, we turn to the full 2-D geometry of Antarctica using the algorithm described in Section 2.3, first by constructing an appropriate effective ocean temperature field from observational data.

3.1 Comparison of basal melt parametrizations along flow lines

Topographic data along flow lines for both Filchner-Ronne ice shelf (FRIS) and Ross ice shelf are taken from Bombosch and Jenkins (1995) and Shabtaie and Bentley (1987), respectively. This data can be used to determine the quantities z_b , α and z_{gl} necessary for calculating the basal melt with the parametrization of Section 2.2. Furthermore, we define a uniform ambient ocean temperature $T_a = -1.9 \text{ }^{\circ}\text{C} + \Delta T$, where ΔT is varied between runs, and a constant ambient ocean salinity $S_a = 34.65 \text{ psu}$. The results of these calculations are shown in Figs. 5 and 6 and compared with those of the full plume model described in Section 2.1. Moreover, we compare with two simple basal melt parametrizations based on Eqs. (1), namely the linear (i.e. in $T_a - T_f$) parametrization by Beckmann and Goosse (2003) with constant γ_T and the quadratic parametrization by DeConto and Pollard (2016) with $\gamma_T = \kappa_T |T_a - T_f|$. Apart from the values listed in Table 1, additional model parameters used for these calculations are given in Table 3.

Figs. 5 and 6 show that both the current parametrization and the original plume model yield approximately the same melt-rate patterns as a function of the horizontal distance from the grounding line. These patterns roughly correspond to the dimensionless melt curve in Fig. 2, i.e. maximum melt near the grounding line and possibly refreezing further away along the flow line. This is most apparent in Fig. 5a, which ~~clearly~~ shows a transition from melting to freezing, since the relatively deep draft of

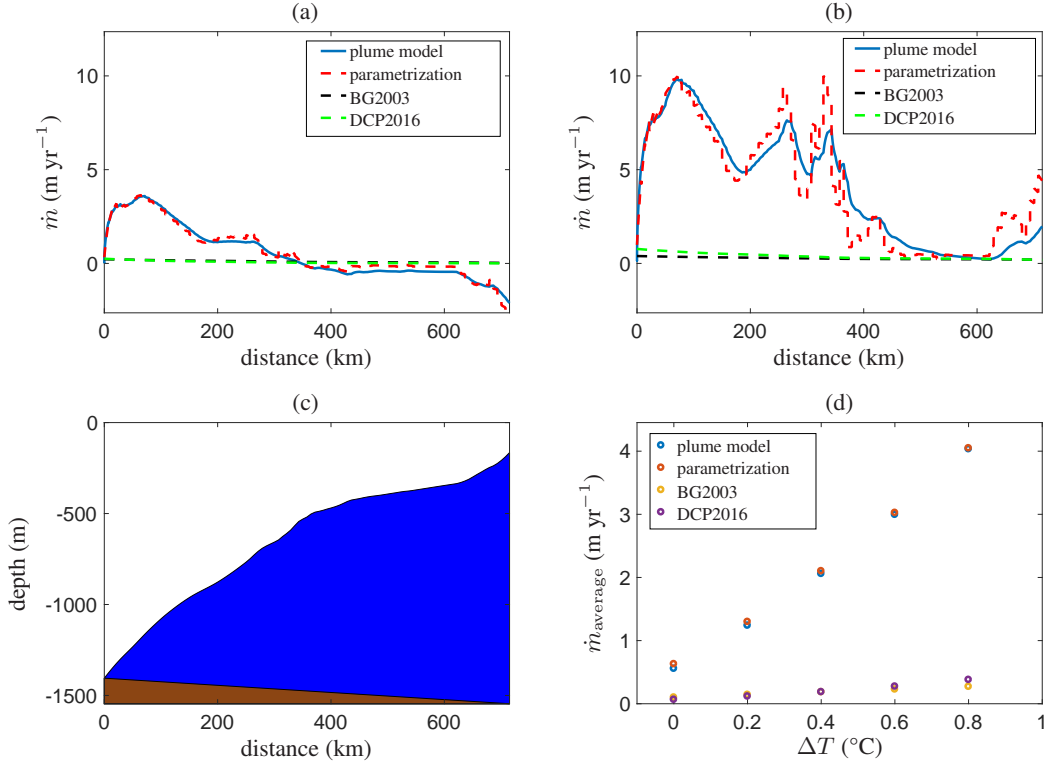


Figure 5. Comparison of the plume model (Section 2.1) with the 1-D basal melt parametrization (Section 2.2), as well as the parametrizations of Beckmann and Goosse (2003) (BG2003) and DeConto and Pollard (2016) (DCP2016), for a flow line along Filchner-Ronne ice shelf with uniform ocean temperature $T_a = -1.9$ °C + ΔT and constant salinity $S_a = 34.65$ psu. (a) Melt pattern for $\Delta T = 0$ °C. (b) Melt pattern for $\Delta T = 0.8$ °C. (c) Geometry of the ice-shelf base. (d) Horizontally averaged melt rates as a function of ΔT .

FRIS allows higher values of the dimensionless coordinate \hat{X} . On the other hand, Fig. 6a does not show refreezing because the draft of Ross ice shelf is much shallower. Increasing the ocean temperature (through ΔT) can significantly enhance basal melt and remove the area of refreezing, as shown in Figs. 5b and 6b. In these cases, additional melt peaks occur in regions of high basal slope. Moreover, although the general agreement is good, the discrepancies between the current parametrization and the plume model are largest when the basal slope changes rapidly, because the parameterization responds immediately to the change while the full model has an inherent lag as the plume adjusts to the new conditions. On the whole, we see that the melt patterns given by the plume parametrization can be quite complex, while the two simple parametrization give nearly constant curves (i.e. independent of the position with respect to the grounding line).

It is interesting to investigate the temperature sensitivity of the four models in terms of the horizontally averaged melt rate as a function of ΔT , as shown in Figs. 5d and 6d. In the case of FRIS, the plume model and parametrization are much more sensitive to the ocean temperature than the two simpler models. However, the average melt rates for Ross ice shelf are rather

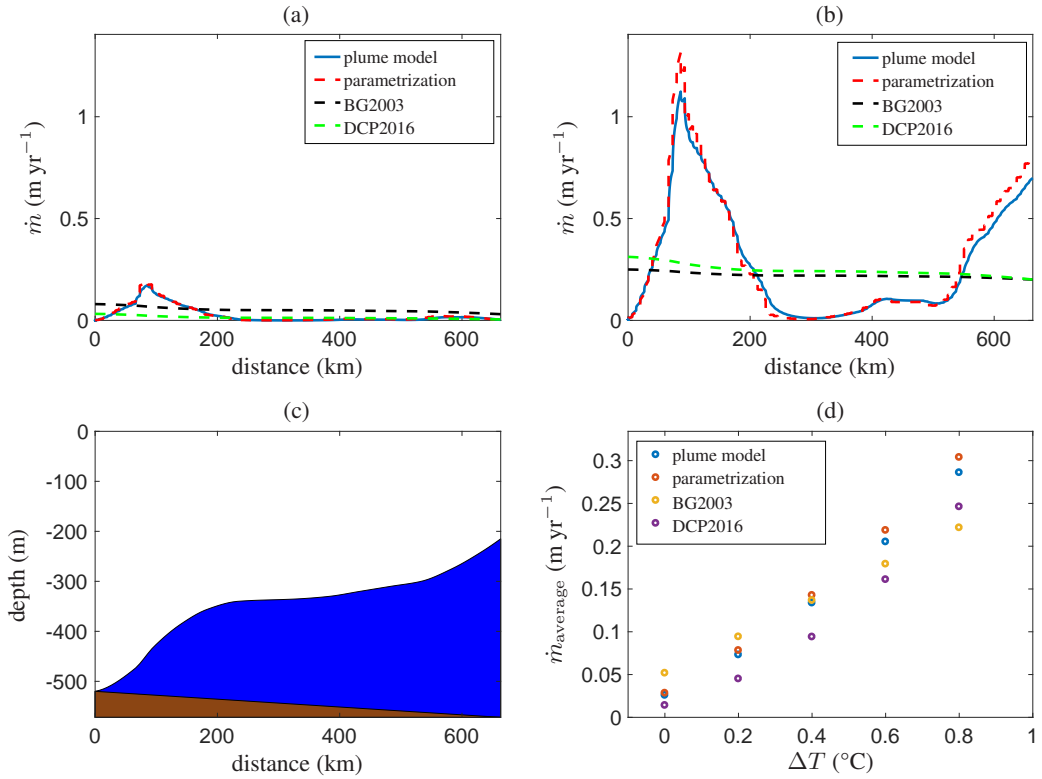


Figure 6. As Fig. 5, but for a flow line along Ross ice shelf.

similar for all four models and all values of ΔT . Hence, the difference in the temperature sensitivity depends significantly on the ice-shelf geometry, where the plume parametrization appears to have a larger potential for capturing diverse melt values than the simpler models. Note that in both cases, the temperature dependence of the plume parametrization is slightly nonlinear, similar to the DeConto and Pollard (2016) parametrization, while the Beckmann and Goosse (2003) parametrization has a linear temperature dependence. Following the discussion of Holland et al. (2008), the temperature dependence of the plume parametrization should therefore be more realistic than the one of Beckmann and Goosse (2003). However, the quadratic parametrization of DeConto and Pollard (2016) tends to significantly underestimate the melt rates as well, despite its nonlinearity. It appears that the geometry dependence of the plume parametrization is an important factor for the temperature sensitivity of the calculated basal melt rates. In Section 3.3 we show that these geometrical effects are indeed crucial for obtaining realistic melt rates with the 2-D parametrization. ~~This also means that the simplest basal melt parametrizations currently used in some ice sheet models, namely constant values or monotonic functions of the water column thickness below the ice shelf, are far from being valid. The latter class of models would even give a gradual increase of melt from the grounding line to~~

~~the ice front, which is opposite to the behaviour of the plume parametrization in Figs. 5 and 6,~~ but first we discuss the matter of determining a suitable input ocean temperature field.

3.2 Effective ocean temperature

The previous section dealt with the 1-D basal melt parametrization along a flow line using a uniform ambient ocean temperature 5 for the entire ice-shelf cavity. While a uniform temperature might appear a reasonable first approximation for a single ice shelf, it is far from realistic to apply a single ocean temperature for multiple ice shelves around the entire Antarctic continent. Therefore, in order to apply the parametrization to the 2-D geometry defined by Fig. 4, a suitable 2-D field for the ocean 10 temperature T_a is required. In principle, the same is true for the salinity S_a , but we will assume that the horizontal variations in ocean salinity around Antarctica are so small that the pressure freezing point T_f is only affected by variations in depth. In 15 the following, we will therefore take a uniform salinity $S_a = 34.6$ psu. One should realize that vertical variations in S_a , which are not accounted for in the current parametrization, would be important in reality, as discussed in Section 4.

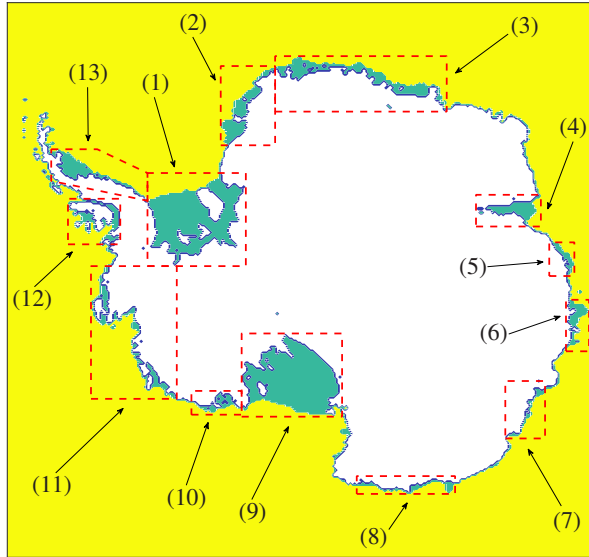
Two problems arise when considering a 2-D ocean temperature field for forcing the parametrization. First of all, such a field should ideally be based on observational data, but ocean temperature measurements in the Antarctic ice-shelf cavities are sparse. ~~The best possibility is A more feasible approach would be to compute~~ an interpolated field based on ocean temperature 15 data in the surrounding ocean, which inevitably contains artefacts resulting from the non-uniform and predominantly summer-time sampling. Secondly, even if a complete dataset of ocean temperatures were available, it is not immediately clear which temperatures (i.e. at which depth) are characteristic for the ocean water reaching the grounding lines (e.g. Jenkins et al. 2010). In principle, detailed knowledge of the bottom topography and the ocean circulation would be required for this, which goes beyond the scope of the current modelling approach.

20 In view of these issues, we construct an *effective ocean temperature* field with which the current plume parametrization yields melt rates that are as close as possible to present-day observations, averaged over entire ice shelves. ~~This approach is based on the rationale that a model with a sufficiently realistic physical basis requires minimally tuned forcing data to produce realistic output. We shall shortly show that this is indeed possible with the plume parametrization. To determine whether the resulting basal melt rates are realistic, In other words, this can be regarded as the inverse problem of computing the unknown~~ 25 ocean temperatures by assuming that the model output for the melt rates matches the (averaged) observations. For this purpose, we use the results of Rignot et al. (2013), who calculated the area-averaged melt rates for each Antarctic ice shelf, based on a combination of observational data and regional climate model output for the different terms in the local ice-shelf mass balance. Other datasets for recent Antarctic basal melt rates exist (e.g. Depoorter et al. 2013), as well as more recent data for 30 ice-shelf thinning (Paolo et al., 2015) from which the basal melt rates can be calculated when combined with the other terms in the mass balance (e.g. velocity and surface melt rates). These alternative datasets for the (area-averaged) basal melt rates are expected to be at least of the same order of magnitude, which we deem sufficient for the purpose of the current study. Since it is impossible to resolve each individual ice shelf from the Rignot et al. (2013) dataset with the currently used 20-km resolution (Fig. 4), we consider a set of 13 ice-shelf groups and determine the area-averaged basal melt for each group from the data of Rignot et al. (2013). The definition of these groups along with the calculated average melt rates are shown in Fig. 7. Note that

the shelves have been grouped based on their geographical location, but also for more practical reasons such as the possibility of distinguishing their boundaries on the 20-km grid.

As a starting point for constructing the effective ocean temperature, we consider the observational data of the World Ocean Atlas 2013 (WOA13, Locarnini et al. 2013), which contains a global dataset of (annual mean) ocean temperatures within a range of depths (0 – 5500 m). Restricting ourselves to the temperature data for latitudes south of 60°S, we average the ocean temperatures over depth intervals $[z_1, z_2]$, where z_1 is the level of the bed (i.e. the deepest level for which data is available) with the additional constraint $z_1 \geq -1000$ m, and $z_2 = \min\{0, z_1 + 400\}$ m. This results in a relatively smooth 2-D temperature field containing an inherent dependence on the bottom topography, which can be considered a first estimate for the ocean water flowing into the ice-shelf cavities. ~~One should note that the details of the depth averaging are rather arbitrary as we will soon modify the temperature field in order to obtain melt rates that agree with the data of Rignot et al. (2013).~~ The depth-averaged temperature field is now remapped on the same 20-km grid as the topography data (see Section 2.3 and Fig. 4) and interpolated using natural-neighbour interpolation (i.e. a weighted version of nearest-neighbour interpolation, giving smoother results) to obtain data in the entire domain of interest. The resulting temperature field, called T_0 , is shown in Fig. 8a. One should note that both the depth-averaging and the interpolation procedures introduce biases in the resulting field. In particular, the rather simple interpolation technique also interpolates ocean temperatures between ice-shelf cavities separated by the continent or grounded ice, which is not realistic as it propagates temperatures into cavities that the corresponding ocean water cannot reach. Using the natural-neighbour interpolation method appears to limit these effects. However, the details of the resulting field T_0 are somewhat arbitrary as it needs to be adjusted in order to obtain melt rates that agree with the data of Rignot et al. (2013).

The aim is now to modify this depth-averaged, interpolated temperature field T_0 in such a way that the basal melt parametrization yields melt rates close to those shown in Fig. 7 for each ice-shelf group. As explained earlier, this modification is necessary for eliminating biases in T_0 caused by the sparse observations and numerical interpolation, and also because the flow dynamics of the ocean are not resolved. The field T_0 is now modified by adding a 2-D field of temperature differences (ΔT), which, in turn, is the result of ~~linearly interpolating~~ linearly interpolating individual values of ΔT in 29 carefully chosen sample points, with $\Delta T = 0$ on the domain boundary. The sample points and values of ΔT have been determined by trial and error and are certainly not a unique nor optimal configuration. The points are mainly located in regions that are most affected by interpolation between strictly separated cavities (e.g. grounding line of FRIS) or extrapolation of warm open-ocean temperatures into cavities (e.g. Dronning Maud Land, shelf groups 2 and 3 in Fig. 7). The resulting effective temperature field, $T_{\text{eff}} = T_0 + \Delta T$, is shown in Fig. 8b, which also indicates the positions of the aforementioned sample points along with the used values of ΔT in these points. Note that for technical reasons explained in Appendix A, we have applied a lower limit to the effective temperature equal to the pressure freezing point at surface level. With the current choice $S_a = 34.6$ psu, this implies $T_{\text{eff}} \geq -1.9$ °C. Comparing Figs. 8a and b, we see that the main effect of ΔT is a decrease in the ocean temperature over most of the continental shelf and most ice-shelf cavities (in particular for Ross and Amery ice shelves), and a slight increase in the ocean temperature in West Antarctica and some regions in East Antarctica (e.g. shelf group 6 in Fig. 7). Again, note that the details in the procedure for calculating T_0 and ΔT are somewhat arbitrary, since increasing one term would require decreasing the other term in order to obtain similar values for T_{eff} with similar basal melt rates.



Ice-shelf group	Average basal melt (m yr^{-1})
1 <i>Filchner, Ronne</i>	0.32 ± 0.08
2 <i>Stancomb, Brunt, Riiser-Larsen, Quar, Ekström, Atka</i>	0.2 ± 0.1
3 <i>Jelbart, Fimbul, Vigrid, Nivl, Lazarev, Borchgrevink, Baudoin, Prince Harald, Shirase</i>	0.5 ± 0.1
4 <i>Amery, Publications</i>	0.6 ± 0.4
5 <i>West</i>	1.7 ± 0.7
6 <i>Shackleton, Tracy, Tremenchus, Conger</i>	2.7 ± 0.5
7 <i>Totten, Moscow University, Holmes</i>	7.1 ± 0.5
8 <i>Mertz, Ninis, Cook East, Rennick, Lillie</i>	1.7 ± 0.4
9 <i>Ross</i>	0.12 ± 0.07
10 <i>Sulzberger, Swinburne, Nickerson, Land</i>	1.5 ± 0.2
11 <i>Getz, Dotsen, Crosson, Thwaites, Pine Island, Cosgrove, Abbot, Ven- able</i>	5.6 ± 0.3
12 <i>Stange, George VI, Bach, Wilkins</i>	3.0 ± 0.4
13 <i>Larsen B-C-D-E-F-G</i>	0.5 ± 0.6

Figure 7. The 13 groups of ice shelves used for constructing the effective ocean temperature field. Average melt rates and error estimates ([one sigma](#)) for each group are calculated from the data of Rignot et al. (2013) for individual ice shelves.

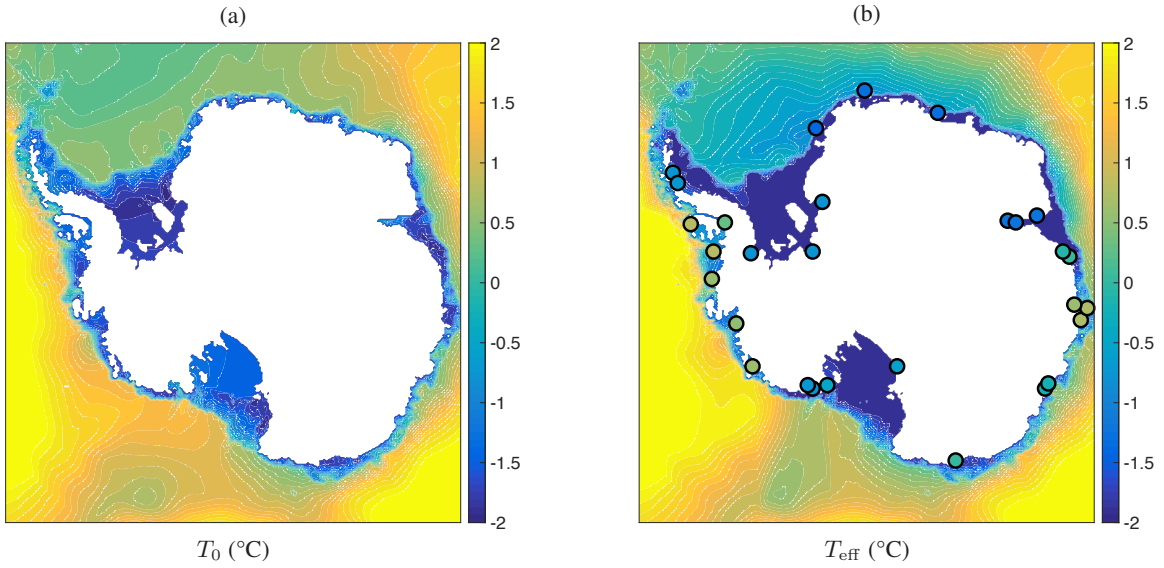


Figure 8. (a) Depth-averaged and interpolated ocean temperature, T_0 , calculated from [annual mean](#) WOA13 data. (b) Effective ocean temperature $T_{\text{eff}} = \max\{T_0 + \Delta T, -1.9\}$ constructed from T_0 as described in Section 3.2. The circles indicate the positions of the sample points in which the values of ΔT are imposed. The colour of each circle corresponds to the imposed value of ΔT (same colour scale), ranging from -1.4 °C to 0.8 °C. The full ΔT field is obtained by linearly interpolating these values.

Fig. 9 shows the basal melt rates computed by the parametrization using the effective temperature T_{eff} of Fig. 8b as forcing. An area-averaged value is obtained for each of the 13 ice-shelf groups in Fig. 7 and compared with the observational values from the Rignot et al. (2013) data. By construction, the modelled basal melt rates correspond closely to the observational values and fall within the error estimates. A notable exception is the value for Filchner-Ronne ice shelf (FRIS), which is 0.32 ± 0.08 5 m yr^{-1} according to the observations, whereas the parametrization gives a value just above 0.5 m yr^{-1} . This discrepancy is caused by the lower bound of -1.9 °C imposed on the effective temperature. As we can see in Fig. 8b, the ocean water below FRIS is almost entirely at this minimum temperature, making it impossible to further improve the basal melt rate without using unfeasibly low values for T_{eff} . ~~The lower bound also has a physical meaning, as the inflow of ocean water into the ice-shelf cavities is unlikely to be much colder than the surface freezing point. This rather technical constraint might be relaxed in various ways, as briefly discussed in Appendix A, possibly improving the melt rates in very cold cavities.~~

Nevertheless, the plume parametrization in conjunction with the constructed effective temperature field appears to yield realistic present-day melt rates for all shelf groups. ~~Therefore, we can conclude that~~ By construction, the effective temperature shown in Fig. 8b ~~is a realistic forcing field, at least within the current modelling framework. Clearly, this field~~ contains an inherent dependence on the bottom topography, with typically lower temperatures above the continental shelves (and thus 15 in the ice-shelf cavities), while still retaining the spatial variation in temperature of the surrounding deep ocean (e.g. higher temperatures for West-Antarctica, leading to higher melt rates for ice-shelf groups 11 and 12 as defined in Fig. 7).

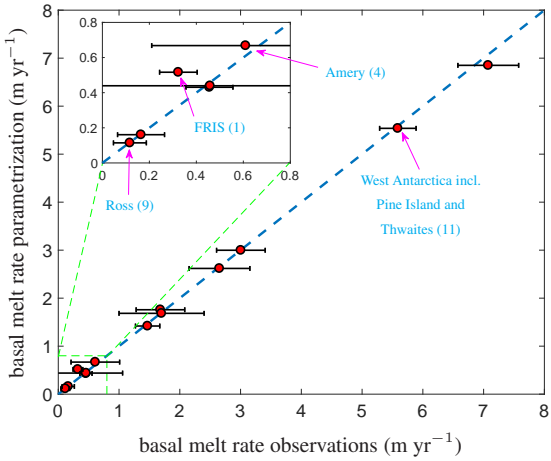


Figure 9. Area-averaged basal melt rates for each ice-shelf group in Fig. 7 obtained with the plume parametrization and the effective temperature field of Fig. 8b. The modelled melt rates are plotted against the averaged observational values given in Fig. 7. For four important shelf groups, the data points are explicitly labelled along with the corresponding group number in Fig. 7. The horizontal error bar is a one sigma uncertainty in the observations.

3.3 Comparison of 2-D melt-rate patterns

The effective grounding-line depth and effective slope in Fig. 4, the effective ocean temperature in Fig. 8b and the assumption $S_a = 34.6$ psu constitute the full set of input parameters necessary for evaluating the plume parametrization on the entire 2-D geometry. The resulting 2-D field of basal melt rates under all Antarctic ice shelves is shown in Fig. 10a (note that this is the same data used for the area-averaged melt rates in Fig. 9, but now plotted as a spatial field rather than averaged values over the ice shelves). A general pattern that can be observed, especially on the bigger ice shelves, consists of regions of higher melt close to the grounding line and lower melt or patches of refreezing closer to the ice front. This pattern is ~~obviously~~ a consequence of the underlying plume model, as shown in Section 3.1 for data along a flow line. Moreover, the highest melt rates occur in West Antarctica (shelf groups 11 and 12) and some specific shelves in East Antarctica (shelf groups 6 and 7), where the ~~constructed~~ effective temperature is significantly higher than elsewhere. ~~This fact, along with the general melt pattern and the correlation with the surrounding ocean temperature, are~~ ~~The general melt patterns within individual cavities appear to be~~ in line with observations, e.g. Rignot et al. (2013). However, one should note that the Rignot et al. (2013) melt pattern shows a greater spatial variability, with more patches of (stronger) refreezing occurring between patches of positive melt. ~~The lack of such prominent patches of refreezing (Fig. 12a). Especially beneath FRIS and Ross ice shelf, the melt pattern appears quite complex and local deviations from the general pattern can be considerable (Fig. 12b). These discrepancies~~ in the current parametrization might have different reasons, such as the coarse resolution or the fact that we disregard the details of the ocean circulation within the ice-shelf cavities, as well as effects due to ~~stratification and~~ the Coriolis force ~~and both seasonal and vertical variability in the temperature and salinity fields~~. ~~All in all, the plume parametrization, together with the effective~~

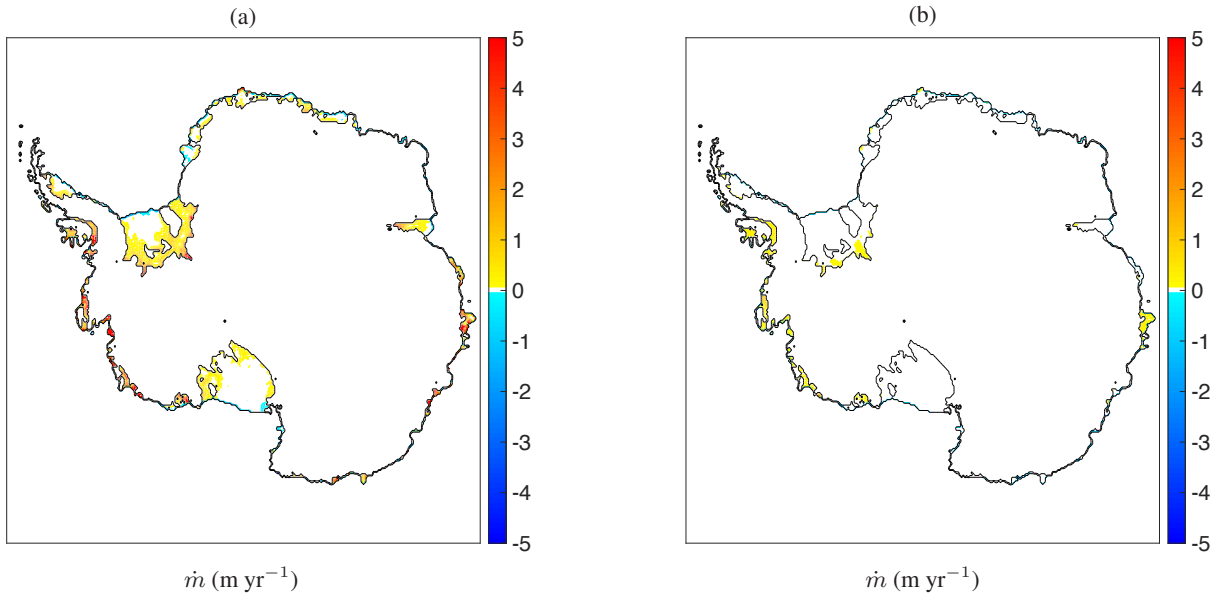


Figure 10. Basal melt rates in meter per year with the Bedmap2 topographic data and the effective temperature field of Fig. 8b as obtained from: (a) the plume parametrization with additional input parameters from Fig. 4; (b) the quadratic parametrization of DeConto and Pollard (2016).

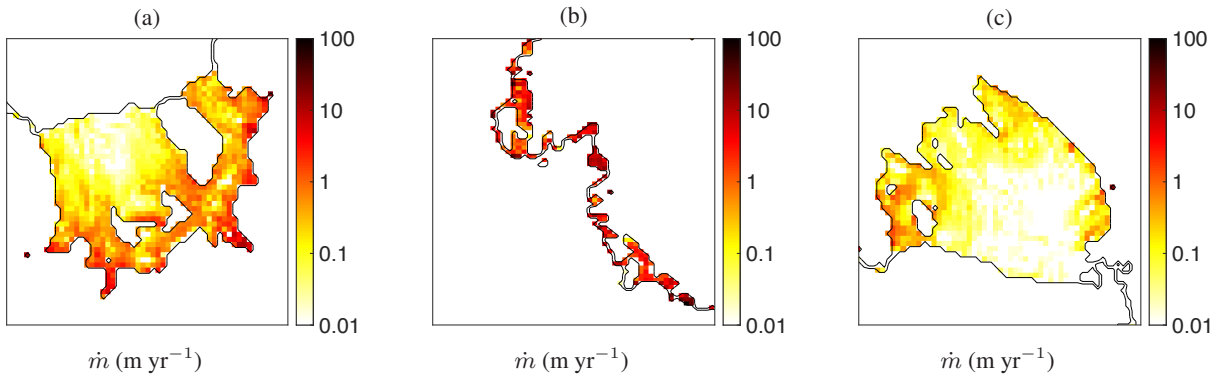


Figure 11. As Fig. 10a, but with a logarithmic color scale (negative and zero values shown white) and zoomed in on important areas: (a) Filchner-Ronne ice shelf (group 1), (b) West Antarctica including Pine Island and Thwaites (group 11), (c) Ross ice shelf (group 9).

~~temperature field, appears to give a realistic melt pattern for Antarctica, showing both a large spatial variability and average melt rates that agree with observations.~~

Furthermore, Figure 10 shows the melt rates patterns of the plume parametrization zoomed in on three important regions, giving more insight in the orders of magnitude of the highest melt rates. The high near-grounding-line melt rates for FRIS have values between 1 and 10 m yr^{-1} , while those for Ross ice shelf appear one order of magnitude smaller. On the other hand, the West Antarctic melt rates shown in Fig. 11b have values around 10 m yr^{-1} or more due to the higher ocean temperatures here.

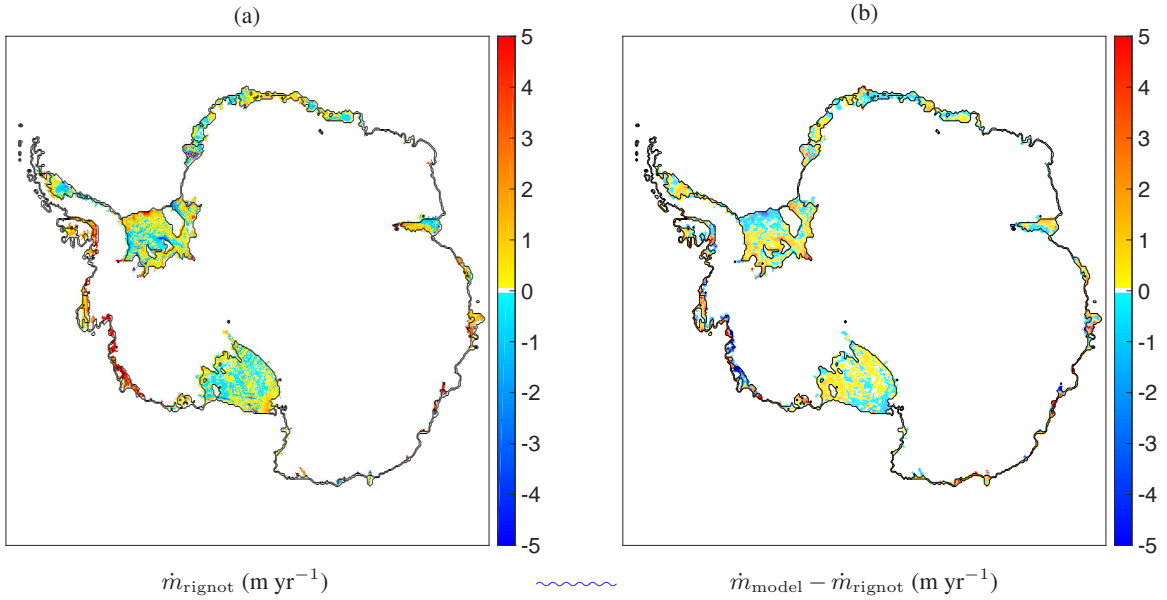


Figure 12. Basal melt rates in meter per year extracted from the Rignot et al. (2013) observational dataset (courtesy of Dr Jeremie Mouginot): (a) raw data plotted together with the currently used mask; (b) difference between the plume parametrization (Fig. 10a) and the observations interpolated on the 20-km grid.

It should be noted, however, that the latter values are still lower than those observed in the Rignot et al. (2013) data, where local melt rates can reach 100 m yr^{-1} .

For comparison, we also evaluate the quadratic parametrization of DeConto and Pollard (2016), described in Section 3.1, using the same geometric data and the effective temperature field of Fig. 8b as input. The resulting basal melt rate pattern is shown in Fig. 10b. Comparing this figure to Fig. 10a ~~immediately~~ shows that the quadratic parametrization yields significantly lower melt rates than the plume parametrization, at least with the current effective temperature as input. The only visible patches of basal melt are located in the aforementioned regions where the ocean temperature is high, as well as near the grounding line of Filchner-Ronne ice shelf. Therefore, if the effective temperature in Fig. 8b is indeed characteristic of the true temperatures in the ice-shelf cavities, the quadratic parametrization would require significant tuning in order to obtain a similar agreement with observed melt rates as currently found with the plume parametrization. For completeness, we mention that the linear parametrization of Beckmann and Goosse (2003) yields even lower melt rates due to its low temperature sensitivity, as discussed in Section 3.1.

To further clarify the differences between the two parametrizations in Fig. 10, we have repeated the steps outlined in Section 3.2 and constructed a second effective temperature field based on the quadratic parametrization by DeConto and Pollard (2016) instead of the plume parametrization. The resulting temperature field is shown in Fig. 13a. Note that the difference between this field and the one in Fig. 8b only lies in the values chosen for ΔT and not in the underlying interpolated observations (T_0). For simplicity, the ΔT values have been imposed in the same sample points as used for Fig. 8b. Comparing the

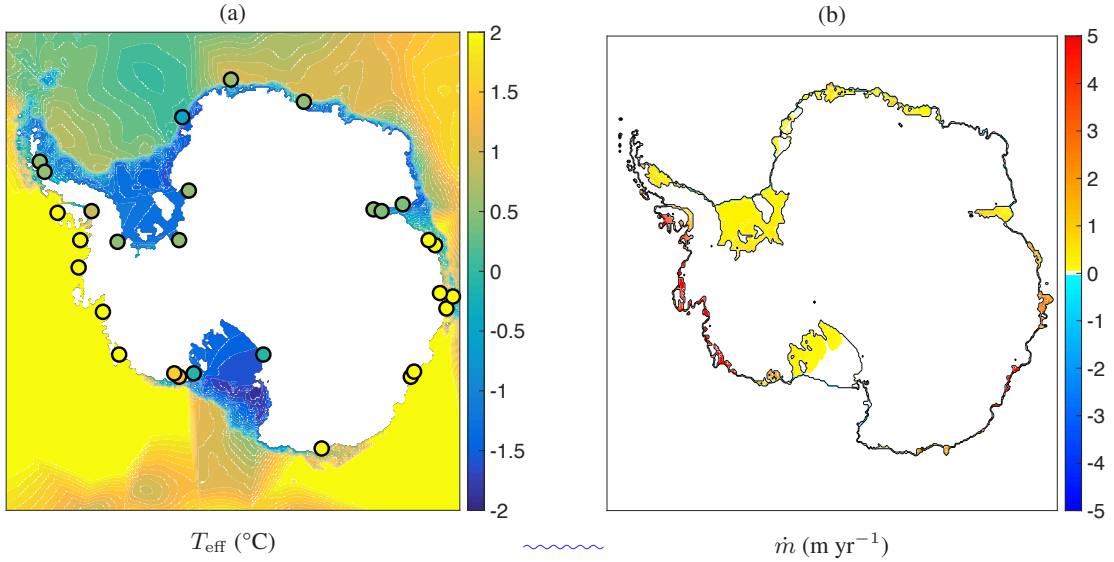


Figure 13. (a) Effective temperature field constructed in a similar way as Fig. 8b, but with different values for ΔT (indicated by the circles and ranging from -0.5°C to 5.4°C), chosen in order to match the melt rates of the quadratic parametrization of DeConto and Pollard (2016) with the data of Rignot et al. (2013). (b) Basal melt rates obtained with the quadratic parametrization of DeConto and Pollard (2016) using the Bedmap2 topographic data and the effective temperature in (a) as input.

two effective temperature fields in Figs. 8b and 13a shows that much higher ocean temperatures are required for the quadratic parametrization to give realistic area-averaged melt rates. The ΔT values imposed in the sample points indicated in Fig. 13a range from -0.5°C to 5.4°C , while those used for Fig. 8b range from -1.4°C to 0.8°C . Furthermore, we can calculate the root mean square values of $T_{\text{eff}} - T_0$ over the entire domain (disregarding the continental points), yielding 0.3°C for Fig. 8b and 1.1°C for Fig. 13a. Hence, the effective temperature in Fig. 8b lies closer to the underlying observational data T_0 than the field in Fig. 13a.

The basal melt rates resulting from the quadratic parametrization and the new effective temperature field are shown in Fig. 13b. Clearly, the higher ocean temperatures cause significantly higher melt rates than those shown in Fig. 10b. However, compared with the plume parametrization in Fig. 10a, the spatial distribution of these melt rates is more uniform, showing less prominent melt peaks near grounding lines and no patches of refreezing. It appears that the quadratic temperature dependence together with the (slight) depth dependence through the pressure freezing point T_f (equation (1b)) is not sufficient for obtaining realistic melt rates without significantly increasing the input ocean temperature, which can be considered equivalent to using different tuning factors for different ice shelves. On the other hand, the plume parametrization, containing an additional geometry dependence through the grounding-line depth and local slope, appears to yield the required melt rates rather naturally with ~~only a minimal tuning of the observed ocean temperatures~~ ~~constructed ocean temperature within a plausible range~~, and it results in a more realistic spatial pattern with highest basal melt rates near the grounding line as well as areas of refreezing.

4 Discussion

The plume parametrization in combination with the 2-D algorithm of Section 2.3 and the effective temperature field of Section 3.2 is able to capture a more complex spatial pattern of basal melt rates and a high temperature sensitivity, which is an important step forward compared to the simpler models based only on Eqs. 1. However, the plume parametrization 5 also relies on several rather strong assumptions, which we discuss below. First of all, both the original plume model and the parametrization have a quasi-1-D formulation, assuming homogeneity in the spanwise direction. Even though we attempt to translate this formulation to two dimensions with the algorithm in Section 2.3, there are undoubtedly errors associated with the underlying 1-D assumptions. As already discussed in Section 2.3, an important 2-D effect is the additional degree of freedom 10 associated with the widening of the plume, which influences the plume dynamics and the melt rates through the mass budget equation (Hattermann, 2012; Hattermann et al., 2014).

Furthermore, the current algorithm for finding the plume paths in 2-D is not unique and more realistic and efficient methods 15 might be possible, e.g. by extrapolating the plume outward from the grounding line instead of searching for surrounding grounding-line points from each shelf point. Also, the current algorithm was developed for the relatively coarse resolution of 20×20 km, suitable for use in an ice-sheet model, and takes into account only the local slope and overall grounding-line depth, whereas higher resolution runs might benefit from a different and more precise method. On the other hand, a higher resolution 20 would also entail a more rapid variation of the basal slope, potentially causing high melt peaks (Section 3.1) that would be smoother in the original plume model. This would introduce the need for a smoothing algorithm for higher resolutions. All in all, the current formulation should be considered as a relatively simple parametrization of the net circulation within an ice-shelf cavity, providing non-local features to the basal melt calculation that are not present in the simpler models. Further work is needed to determine whether the realism of the current formulation can be improved.

Another very important feature that has been neglected in the derivation is the vertical variation in the temperature and 25 salinity fields. In reality, stratification and the existence of different water masses have a crucial effect on plume buoyancy, e.g. by causing the plume to detach from the ice-shelf base at levels of neutral buoyancy. As explained in Sec. 2.2, the current formulation is based on the assumption that the freezing-point length scale (9) is dominant w.r.t. the length scale 30 associated with stratification, as well as those associated with rotation and the initial meltwater flux at the grounding line. This assumption indeed works well in conjunction with constant values for T_a and S_a , describing a net circulation for which the buoyancy is parametrized in terms of $T_a - T_f$, as shown more precisely in Appendix A. In this framework, the values of T_a and S_a determine the overall magnitude of plume buoyancy, while the variation along the plume path is described by the depth-dependence of the freezing point T_f . This is also the reason why the small horizontal variations in S_a have only a small effect on the overall buoyancy and can be neglected, as was done in Section 3. However, for obtaining a fully realistic melt rate 35 pattern it will be important to also include the effects of vertical and seasonal variations in T_a and S_a , e.g. in order to capture seasonal intrusion of warmer surface waters (mode 3 melting; Jacobs et al. 1992; Hattermann et al. 2012; Stern et al. 2013).

An important uncertainty in the current study is the construction of the effective temperature field (Section 3.2). In principle, this is done due to the lack of detailed ocean temperature observations beneath the ice shelves. One should note, however, that

in attempting to eliminate the biases caused by the sparse data, we are also correcting for errors in the parametrization itself, since the construction is done by constraining the modelled melt rates. In this respect, the *effective* temperature field (or more precisely, ΔT) should be regarded as part of the modelling framework. It would be crucial for the complete validation of the model to perform additional temperature sensitivity studies to see how the plume parametrization might respond to an evolving ocean. Ideally, this is done in the context of a coupled ice-ocean model. On the large scales currently considered, lack of detail within the ice-shelf cavities will likely remain a problem also when using an ocean general circulation model. Since the current formulation is based on constant ocean properties within individual cavities, a method to determine T_{eff} from an ocean model could be extrapolating the model temperature within a characteristic depth-range at the ice front and using a (possibly different) ΔT to constrain the output melt rate, similar to the construction presented here.

On a more technical note, the current construction of T_{eff} was not based on a sophisticated optimization algorithm, but it is merely a simple method to determine an essentially spatially variable field directly from the observations. An alternative method, which might be more consistent with the derivation of the parametrization, would be to introduce separate values for the ocean temperature for each individual cavity, as the ambient temperature in the current context represents the net inflow into the cavity and not the temperature of meltwater that is produced or mixed locally. On the other hand, the current method is more generic in the sense that it removes the need for defining individual cavities in the model once ΔT (i.e. the constraint on the melt rates) has been determined. It should be noted that the current method using only 29 sample points might become problematic in dynamical simulations that include grounding-line retreat. Hence, in such a context a more sophisticated method might be necessary. Furthermore, it is not yet clear if a fixed ΔT is a realistic assumption for an evolving ocean, and introducing the aforementioned additional variations of T_o and S_o might require different considerations altogether.

Finally, it is interesting to note the existence of alternative methods for describing the net circulation within the ice-shelf cavities. A recent example is a box model that simulates the upward flow under the ice shelf in a similar quasi-1-D context by describing the fluxes of heat and salt between a limited number of predefined boxes (Olbers and Hellmer, 2010). This method has recently been extended to two dimensions and coupled to an ocean model (Reese et al., 2017), yielding Antarctic basal melt patterns similar to the ones given by the plume parametrization. Both methods are similar in the sense that they essentially describe the same type of physical process while not accounting for features such as stratification and 2-D effects, as discussed above. One could argue that a systematically derived approximation to the governing equations is preferred over a simple box model. On the other hand, a box model might be easier to implement and produce similar results in a more efficient way. A more detailed comparison of these two methods is beyond the scope of this work.

5 Conclusions

In this study, we have presented the application of a basal melt parametrization, based on the dynamics of buoyant meltwater plumes, to all ice shelves in Antarctica. The physical basis of this parametrization is the plume model of Jenkins (1991), which describes the fluxes of mass, momentum, heat and salinity within a meltwater plume travelling up from the grounding line along the ice-shelf base. Details of the proposed parametrization have been discussed in earlier works (Jenkins, 2011, 2014)

for idealized one-dimensional geometries along an ice-shelf flow line. In particular, the basal melt rate given by the plume model follows a rather universal scaling law depending on the ice-shelf geometry (basal depth z_b , local slope angle α , and grounding-line depth z_{gl}) as well as the ambient ocean temperature T_a and the pressure freezing point T_f .

Here, the plume parametrization has been tested for two realistic ice-shelf geometries along a flow line and, for the first time, 5 applied to a completely two-dimensional geometry covering all the Antarctic ice shelves. The one-dimensional tests along flow lines of Filchner-Ronne and Ross ice shelves (Section 3.1) reveal the typical characteristics of the parametrization, namely higher melt rates near the grounding line and in regions of high basal slope. Patches of refreezing can occur further away from the grounding line. Moreover, the plume parametrization exhibits a nonlinear dependence on the ocean temperature, and the increase in melting resulting from higher ocean temperature is dependent on the ice-shelf geometry. In contrast, simpler 10 parametrizations based solely on the local balance of heat at the ice-ocean interface are not able to capture the complex melt pattern nor the temperature sensitivity.

Applying the essentially one-dimensional plume parametrization to a two-dimensional geometry is not trivial and, ideally, it would require a detailed knowledge of both the ice-shelf geometry and the ocean circulation in the ice-shelf cavities. The method discussed in Section 2.3 provides a solution to ~~these issues this issue~~ by constructing a field of effective grounding-line 15 depths and slope angles for each shelf point from topographic data. The resulting values for z_{gl} and α can be interpreted as reflecting the average effect of all plumes that reach the shelf point. This method provides a straightforward way to extend the parametrization from 1-D to 2-D for a given topography and ice mask, but it is not unique. ~~For example, it does not directly take into account the horizontal distance from an ice-shelf point to the grounding line (an alternative method presented in Appendix ?? does take this distance into account, without improving the results)~~ As discussed in the previous section, a fully 20 realistic 2-D formulation of the plume dynamics would require additional considerations.

However, since the temperature sensitivity of the plume parametrization can be considerable, a more important factor for the two-dimensional model is finding an ocean temperature field that is characteristic for the ocean water flowing into the ice-shelf cavities. In this respect, the results in Sections 3.2 and 3.3 show that the depth-averaged and interpolated data from observations ~~only need a minimal require a plausible~~ offset ΔT (between -1.4 °C and 0.8 °C) in order to obtain an effective 25 temperature T_{eff} (Fig. 8b) with which the plume parametrization gives basal melt rates close to the present-day observations of Rignot et al. (2013). In contrast, a much higher offset ΔT (between -0.5 °C to 5.4 °C) is required for obtaining the same melt 30 rates with the quadratic parametrization of DeConto and Pollard (2016), as shown in Fig. 13. ~~The latter behaviour~~ The same low temperature sensitivity of the melt rates from the latter parametrization is also apparent in Pollard and DeConto (2012), where different tuning factors in the basal melt parametrization are used for different sectors along the Antarctic coastline, 35 and in DeConto and Pollard (2016), where offsets of 3 °C and 5 °C are added to the ocean temperature in the Amundsen and Bellinghausen seas (resulting from an ocean model) in order to obtain the correct present-day basal melt rates and grounding-line retreat.

All in all, the presented plume parametrization, together with the constructed effective temperature field, gives ~~realistic reasonable~~ results for the spatial pattern of present-day basal melt in Antarctica, ~~both in terms of area-averaged values (Fig. 9) and the spatial pattern (Fig. 10a).~~ The inherent geometry dependence, based on the plume dynamics, gives a more natural

spatial variation that cannot be captured with local heat-balance models, a major aspect being the occurrence of refreezing. Of course, the current discussion only assumes a steady state regarding the ice dynamics and the ocean temperature. The question remains how an ice-dynamical model would behave when coupled to the plume parametrization, both for present-day forcing and for a varying climate. As a next step, it is important to perform such transient simulations of an ice model 5 coupled to the plume parametrization and conduct sensitivity experiments. For such simulations, the effective temperature in Fig. 8b, even though it is a constructed field, can prove to be a valuable reference state to which temperature anomalies can be added—as briefly discussed in Section 4. Eventually, coupled ice-ocean simulations (e.g. DeConto and Pollard 2016) ~~can~~ might benefit from this approach by ~~comparing using both~~ ocean-model output ~~to~~ and this reference state to determine an appropriate temperature forcing for this type of basal melt parametrizations.

10 Appendix A: Details of the basal melt parametrization

Here we present more details of the basal melt parametrization summarized in Section 2.2, starting with the theoretical arguments behind its mathematical form. The precise form of the parametrization is, however, the result of an empirical study of the plume model results (Jenkins, 2014) and described at the end of this appendix.

First of all, we consider a simplified form of the plume equations (2)-(4), (6), where we neglect all advection terms except the 15 crucial mass flux $\Phi_m := \frac{dDU}{dX}$, since without this flux there would be no plume. Furthermore, we replace the salinity equation by an equation for the density contrast $\Delta\rho$ as defined in (4) (similar to Jenkins 2011), neglect the direct effect of the melt rate \dot{m} in the mass equation w.r.t. the entrainment flux (retaining it only for the heat and buoyancy fluxes), neglect heat conduction into the ice in the ice-ocean interface condition, and take $S_i = 0$. In the case of constant ocean properties (T_a, S_a) , as considered also for the empirical derivation of the plume parametrization, this set of assumptions yields the following simplified system:

$$20 \quad \Phi_m = E_0 U \sin \alpha, \quad (\text{A1a})$$

$$\Phi_m U = D \frac{\Delta\rho}{\rho_0} g \sin \alpha - C_d U^2, \quad (\text{A1b})$$

$$\Phi_m T = (E_0 U \sin \alpha) T_a + \dot{m} T_f - C_d^{1/2} \Gamma_{TS} U (T - T_f), \quad (\text{A1c})$$

$$\Phi_m \frac{\Delta\rho}{\rho_0} = \beta_S \dot{m} S_a - \beta_T \dot{m} (T_a - T_f) - \beta_T C_d^{1/2} \Gamma_{TS} U (T - T_f), \quad (\text{A1d})$$

$$\frac{L}{c_w} \dot{m} = C_d^{1/2} \Gamma_{TS} U (T - T_f), \quad (\text{A1e})$$

$$25 \quad T_f = \lambda_1 S + \lambda_2 + \lambda_3 z_b. \quad (\text{A1f})$$

This is an algebraic system that can be solved rather easily for $(U, T, \Delta\rho, \dot{m})$ as functions of the ambient properties (T_a, S_a) , the freezing point T_f and the basal slope angle α . The solution can be written compactly as follows:

$$\dot{m} = C_d^{1/2} \Gamma_{TS} \cdot U \cdot \left(\frac{\Delta T}{L/c_w} \right), \quad (\text{A2a})$$

$$U = (gD\Delta\rho)^{1/2} \cdot \left(\frac{\sin \alpha}{C_d + E_0 \sin \alpha} \right)^{1/2}, \quad (\text{A2b})$$

$$5 \quad \Delta T = T - T_f = \left(\frac{E_0 \sin \alpha}{C_d^{1/2} \Gamma_{TS} + E_0 \sin \alpha} \right) \cdot (T_a - T_f), \quad (\text{A2c})$$

$$\Delta\rho = \left(\frac{C_d^{1/2} \Gamma_{TS}}{E_0 \sin \alpha} \right) \left(\frac{\Delta T}{L/c_w} \right) Q_0^2(T_a, T_f, S_a), \quad (\text{A2d})$$

with

$$Q_0(T_a, T_f, S_a) = \sqrt{\beta_S S_a - \beta_T \left(\frac{L}{c_w} + T_a - T_f \right)} \quad (\text{A2e})$$

By substituting the expressions above in (A2a), we obtain three geometrical factors in the melt rate expression, corresponding 10 to the factor $g(\alpha)$ in the melt scale (8):

$$g(\alpha) = \left(\frac{\sin \alpha}{C_d + E_0 \sin \alpha} \right)^{1/2} \left(\frac{C_d^{1/2} \Gamma_{TS}}{C_d^{1/2} \Gamma_{TS} + E_0 \sin \alpha} \right)^{1/2} \left(\frac{E_0 \sin \alpha}{C_d^{1/2} \Gamma_{TS} + E_0 \sin \alpha} \right) \quad (\text{A3})$$

What remains is to find the required quadratic temperature dependence in (8). First note that the factor Q_0 , essentially determining the magnitude of buoyancy, can be taken approximately constant for constant S_a and $T_a - T_f \ll L/c_w$, which is a reasonable assumption with the values in Table 3. Second, the expressions in (A2) depend on the plume thickness D , which is still an unknown variable. However, for a simple geometry with a constant and small slope α and slowly varying 15 $U(X)$, the plume thickness can be explicitly solved from the mass equation (A1a) and directly related to the depth difference and, hence, the temperature difference:

$$D = E_0(\sin \alpha)X \approx E_0(z_b - z_{gl}) = E_0 \cdot l \cdot \hat{X} \sim (T_a - T_{f,gl})\hat{X}, \quad (\text{A4})$$

where we have used (9) to incorporate the length scale and the dimensionless coordinate \hat{X} . A linear thickening of the plume 20 is indeed a reasonable approximation for a constant slope that is also seen in the plume model output, with slight deviations when the plume decelerates. Third, the temperature differences $T_a - T_f$ and $T_a - T_{f,gl}$ are related in a rather straightforward way:

$$T_a - T_f = T_a - T_{f,gl} - \lambda_3(z_b - z_{gl}) = (T_a - T_{f,gl}) \left(1 - \frac{\lambda_3(z_b - z_{gl})}{T_a - T_{f,gl}} \right) \approx (T_a - T_{f,gl}) \left(1 - \hat{X} \right) \quad (\text{A5})$$

Using (A4) and (A5) in (A2) now yields the following dependence for the melt rate:

$$\dot{m} \sim U \Delta T \sim D^{1/2} \Delta \rho^{1/2} \Delta T \sim D^{1/2} \Delta T^{3/2} \sim D^{1/2} (T_a - T_f)^{3/2} \sim (T_a - T_{f,gl})^2 \cdot \hat{X}^{1/2} (1 - \hat{X})^{3/2}, \quad (\text{A6})$$

which is the required quadratic dependence on $T_a - T_{f,gl}$.

In summary, we have shown how the assumption of a simple geometry with constant slope and constant ocean properties in the simplified system (A1) leads to the form of the melt rate scale (8). As a consequence of the derivation, we also found a relation $\dot{m} \sim \hat{X}^{1/2} (1 - \hat{X})^{3/2}$, showing how the melt rate rather naturally depends on the scaled coordinate \hat{X} defined in (9) (disregarding the factor $f(\alpha)$ for the moment; see below). However, this particular function of \hat{X} does not correspond to the general melt curve in Fig. 2. In particular, it only yields positive values for $0 < \hat{X} < 1$ and does not capture refreezing. The message is that at this point, although we can formally derive the melt rate scale M with the correct temperature and slope dependence, it is still necessary to do an empirical scaling of the plume model results in order to obtain the correct function of \hat{X} . This empirical "fine-tuning" then leads to the exact form of the parametrization described below, including parameters M_0 , x_0 , γ_1 , γ_2 as well as the polynomial fit of $\hat{M}(\hat{X})$. A more thorough analysis of the plume equations would be required to derive the correct form of the melt curve in a similar way as sketched here, possibly including more physical phenomena that were neglected here, such as stratification.

The precise form of the parametrization can now be described as follows. For a given point at the ice-shelf base with local depth z_b and local slope angle α , we can determine the corresponding grounding-line depth z_{gl} and ambient ocean properties T_a and S_a . As summarized in Table 1, these quantities, together with a set of constant parameters, serve as the input of the parametrization. The basal melt rate \dot{m} in meter per year at the particular ice-shelf point is now calculated as follows. First we define the characteristic freezing point:

$$T_{f,gl} = T_f(S_a, z_{gl}) = \lambda_1 S_a + \lambda_2 + \lambda_3 z_{gl}, \quad (\text{A7})$$

and an empirically derived effective heat exchange coefficient Γ_{TS} essentially depending on plume temperature, as discussed in Sec. 2.2:

$$\Gamma_{TS} = \Gamma_T \left(\underbrace{0.545 \gamma_1 + 3.5^{-5} \gamma_2}_{\text{an empirically derived effective heat exchange coefficient}} \cdot \frac{T_a - T_f}{\lambda_3} \frac{T_a - T_{f,gl}}{\lambda_3} \cdot \frac{E_0 \sin \alpha}{\Gamma_{TS0} + E_0 \sin \alpha} \frac{E_0 \sin \alpha}{C_d^{1/2} \Gamma_{TS0} + E_0 \sin \alpha} \right). \quad (\text{A8})$$

The empirically derived melt rate scale M in meter per year (Eq. (8)) is now calculated from:

$$M = \underbrace{10 M_0}_{\text{an empirically derived melt rate scale}} \cdot (T_a - T_{f,gl})^2 \left(\frac{\sin \alpha}{C_d + E_0 \sin \alpha} \right)^{1/2} \left(\frac{\Gamma_{TS}}{\Gamma_{TS} + E_0 \sin \alpha} \frac{C_d^{1/2} \Gamma_{TS}}{C_d^{1/2} \Gamma_{TS} + E_0 \sin \alpha} \right)^{1/2} \left(\frac{E_0 \sin \alpha}{\Gamma_{TS} + E_0 \sin \alpha} \frac{E_0 \sin \alpha}{C_d^{1/2} \Gamma_{TS} + E_0 \sin \alpha} \right)^{1/2} \quad (\text{A9})$$

Table A1. Coefficients for the polynomial fit of the dimensionless melt curve $\hat{M}(\hat{X})$.

p_{11}	6.388×10^4
p_{10}	-3.521×10^5
p_9	8.467×10^5
p_8	-1.166×10^6
p_7	1.015×10^6
p_6	-5.820×10^5
p_5	2.219×10^5
p_4	-5.564×10^4
p_3	8.927×10^3
p_2	-8.952×10^2
p_1	5.528×10^1
p_0	1.371×10^{-1}

The indeed having the general form derived at the beginning of this appendix. Furthermore, the length scale l (Eq. (9)) is given by:

$$l = \frac{T_a - T_f}{\lambda_3} \frac{T_a - T_{f,gl}}{\lambda_3} \cdot \frac{x_0 \Gamma_{TS} + E_0 \sin \alpha}{x_0(\Gamma_{TS} + E_0 \sin \alpha)} \frac{x_0 C_d^{1/2} \Gamma_{TS} + E_0 \sin \alpha}{x_0(C_d^{1/2} \Gamma_{TS} + E_0 \sin \alpha)}, \quad (\text{A10})$$

where the second factor, corresponding to $f(\alpha)$ in (9), provides a slope-dependent scaling of the point of transition between melting ($\dot{m} > 0$) and refreezing ($\dot{m} < 0$) with $x_0 = 0.56$ (see Fig. 2), as discussed in Sec. 2.2. The empirically derived dimensionless scaling factor $x_0 = 0.56$ ensures that the transition point occurs at the same dimensionless position for all plume model results. We can now determine the dimensionless coordinate:

$$\hat{X} = \frac{z_b - z_{gl}}{l}, \quad (\text{A11})$$

and calculate the basal melt rate from:

$$10 \quad \dot{m} = M \cdot \hat{M}(\hat{X}), \quad (\text{A12})$$

where $\hat{M}(\hat{X})$ is the dimensionless melt curve shown in Fig. 2 and given by the following polynomial function:

$$\hat{M}(\hat{X}) = \sum_{k=0}^{11} p_k \hat{X}^k, \quad (\text{A13})$$

for which the coefficients p_k are given in Table A1.

Note that we require $0 \leq \hat{X} \leq 1$ in order to remain within the valid domain of the polynomial fit and avoid unbounded values of \hat{M} . It is rather straightforward to show that $\hat{X} \leq 1$ is guaranteed for $T_a \geq \lambda_1 S_a + \lambda_2$, i.e. the ocean temperature

should be above the freezing point at surface level ($z = 0$). By combining equations (A7), (A10) and (A11) and taking the limit $T_a \rightarrow \lambda_1 S_a + \lambda_2$, we obtain $\hat{X} \rightarrow (1 - z_b/z_{gl})F^{-1}$, where F denotes the second (slope-dependent) factor in (A10). Because all the terms appearing in this factor F are positive and $x_0 < 1$, we have $F \geq 1$. Together with $z_{gl} \leq z_b \leq 0$, this implies $\hat{X} \leq 1$ in this particular limit for the ocean temperature. Since T_a appears in the denominator of \hat{X} in (A11), ocean temperatures above 5 this limit will yield smaller values for \hat{X} . Hence, the $\hat{X} \leq 1$ is guaranteed for $T_a \geq \lambda_1 S_a + \lambda_2$. Note that this is the reason why we have applied this lower limit to the effective temperature T_{eff} in Fig. 8b. The physical reason for the constraint $\hat{X} \leq 1$ is that the plume has lost momentum beyond this value (see Jenkins 2011). Alternatives for constraining the temperature could therefore be forcing $\dot{m} = 0$ for $\hat{X} > 1$ (which would, however, lead to a discontinuity in the melt curve in Fig. 2) or simply forcing $\hat{X} \leq 1$ explicitly.

10 **Appendix B: Alternative algorithm for finding the grounding line depths and slopes**

Competing interests. The authors declare that they have no conflict of interest.

Acknowledgements. The authors thank Dr Jeremie Mouginot for providing the spatial data of basal melt rates from Rignot et al. (2013). Financial support for W.M.J. Lazeroms was provided by the Netherlands Organisation for Scientific Research (NWO-ALW-Open 824.14.003). The lead author wishes to acknowledge the hospitality of Eindhoven University of Technology where part of the work was done.

15 References

Asay-Davis, X. S., Cornford, S. L., Galton-Fenzi, B. K., Gladstone, R. M., Gudmundsson, G. H., Holland, D. M., Holland, P. R., and Martin, D. F.: Experimental design for three interrelated marine ice sheet and ocean model intercomparison projects: MISMIP v. 3 (MISMIP+), ISOMIP v. 2 (ISOMIP+) and MISOMIP v. 1 (MISOMIP1), *Geosci. Model Dev.*, 9, 2471, 2016.

Beckmann, A. and Goosse, H.: A parameterization of ice shelf-ocean interaction for climate models, *Ocean modelling*, 5, 157–170, 2003.

Bo Pedersen, F.: Dense bottom currents in rotating ocean, *J. Hydraul. Div. Amer. Soc. Civ. Eng.*, 106, 1291–1308, 1980.

Bombosch, A. and Jenkins, A.: Modeling the formation and deposition of frazil ice beneath Filchner-Ronne Ice Shelf, *J. Geophys. Res. Oceans*, 100, 6983–6992, 1995.

De Boer, B., Dolan, A. M., Bernales, J., Gasson, E., Goelzer, H., Golledge, N., Sutter, J., Huybrechts, P., Lohmann, G., Rogozhina, I., Abe-5 Ouchi, A., Saito, F., and van de Wal, R.: Simulating the Antarctic ice sheet in the Late-Pliocene warm period: PLISMIP-ANT, an ice-sheet model intercomparison project, *The Cryosphere*, 9, 881–903, 2015.

DeConto, R. M. and Pollard, D.: Contribution of Antarctica to past and future sea-level rise, *Nature*, 531, 591–597, 2016.

Depoorter, M. A., Bamber, J. L., Griggs, J. A., Lenaerts, J. T. M., Ligtenberg, S. R. M., Van den Broeke, M. R., and Moholdt, G.: Calving fluxes and basal melt rates of Antarctic ice shelves, *Nature*, 502, 89–92, 2013.

10 Ellison, T. H. and Turner, J. S.: Turbulent entrainment in stratified flows, *J. Fluid Mech.*, 6, 423–448, 1959.

Fretwell, P., Pritchard, H. D., Vaughan, D. G., Bamber, J. L., Barrand, N. E., Bell, R., Bianchi, C., Bingham, R. G., Blankenship, D. D., Casassa, G., Catania, G., Callens, D., Conway, H., Cook, A. J., Corr, H. F. J., Damaske, D., Damm, V., Ferraccioli, F., Forsberg, R., Fujita, S., Gim, Y., Gogineni, P., Griggs, J. A., Hindmarsh, R. C. A., Holmlund, P., Holt, J. W., Jacobel, R. W., Jenkins, A., Jokat, W., Jordan, T., King, E. C., Kohler, J., Krabill, W., Riger-Kusk, M., Langley, K. A., Leitchenkov, G., Leuschen, C., Luyendyk, B. P., Matsuoka, K., 15 Mouginot, J., Nitsche, F. O., Nogi, Y., Nost, O. A., Popov, S. V., Rignot, E., Rippin, D. M., Rivera, A., Roberts, J., Ross, N., Siegert, M. J., Smith, A. M., Steinhage, D., Studinger, M., Sun, B., Tinto, B. K., Welch, B. C., Wilson, D., Young, D. A., Xiangbin, C., and Zirizzotti, A.: Bedmap2: improved ice bed, surface and thickness datasets for Antarctica, *The Cryosphere*, 7, 375–393, 2013.

Golledge, N. R., Kowalewski, D. E., Naish, T. R., Levy, R. H., Fogwill, C. J., and Gasson, E. G. W.: The multi-millennial Antarctic commitment to future sea-level rise, *Nature*, 526, 421–425, 2015.

20 Hattermann, T.: Ice shelf - ocean interaction in the Eastern Weddell Sea, Antarctica, Ph.D. thesis, UiT, The Arctic University of Norway, Tromsø, available online: <http://hdl.handle.net/10037/5147>, 2012.

Hattermann, T., Nøst, O. A., Lilly, J. M., and Smedsrød, L. H.: Two years of oceanic observations below the Fimbul Ice Shelf, Antarctica, *Geophys. Res. Lett.*, 39, 2012.

Hattermann, T., Smedsrød, L. H., Nøst, O. A., Lilly, J. M., and Galton-Fenzi, B. K.: Eddy-resolving simulations of the Fimbul Ice Shelf 25 cavity circulation: Basal melting and exchange with open ocean, *Ocean Modelling*, 82, 28–44, 2014.

Holland, D. M. and Jenkins, A.: Modeling thermodynamic ice-ocean interactions at the base of an ice shelf, *J. Phys. Oceanogr.*, 29, 1787–1800, 1999.

Holland, P. R., Jenkins, A., and Holland, D. M.: The response of ice shelf basal melting to variations in ocean temperature, *J. Clim.*, 21, 2558–2572, 2008.

30 Jacobs, S. S., Helmer, H. H., Doake, C. S. M., Jenkins, A., and Frolich, R. M.: Melting of ice shelves and the mass balance of Antarctica, *Journal of Glaciology*, 38, 375–387, 1992.

Jenkins, A.: A one-dimensional model of ice shelf-ocean interaction, *J. Geophys. Res. Oceans*, 96, 20 671–20 677, 1991.

Jenkins, A.: Convection-driven melting near the grounding lines of ice shelves and tidewater glaciers, *J. Phys. Oceanogr.*, 41, 2279–2294, 2011.

35 Jenkins, A.: Scaling laws for the melt rate and overturning circulation beneath ice shelves derived from simple plume theory, in: EGU General Assembly 2014, vol. 16 of *Geophysical Research Abstracts*, EGU2014-13755, 2014.

Jenkins, A., Nicholls, K. W., and Corr, H. F. J.: Observation and parameterization of ablation at the base of Ronne Ice Shelf, Antarctica, *J. Phys. Oceanogr.*, 40, 2298–2312, 2010.

Lane-Serff, G. F.: On meltwater under ice shelves, *J. Geophys. Res. Oceans*, 100, 6961–6965, 1995.

Locarnini, R. A., Mishonov, A. V., Antonov, J. I., Boyer, T. P., Garcia, H. E., Baranova, O. K., Zweng, M. M., Paver, C. R., Reagan, J. R., Johnson, D. R., Hamilton, M., and Seidov, D.: World Ocean Atlas 2013, Volume 1: Temperature, NOAA Atlas NESDIS, 73, 2013.

5 MacAyeal, D. R.: Evolution of tidally triggered meltwater plumes below ice shelves, in: *Oceanology of the Antarctic Continental Shelf*, edited by Jacobs, S., pp. 133–143, American Geophysical Union, 1985.

Magorrian, S. J. and Wells, A. J.: Turbulent plumes from a glacier terminus melting in a stratified ocean, *J. Geophys. Res. Oceans*, 121, 4670–4696, 2016.

McPhee, M. G.: Turbulent heat flux in the upper ocean under sea ice, *J. Geophys. Res. Oceans*, 97, 5365–5379, 1992.

10 McPhee, M. G., Kottmeier, C., and Morison, J. H.: Ocean heat flux in the central Weddell Sea during winter, *J. Phys. Oceanogr.*, 29, 1166–1179, 1999.

Morton, B. R., Taylor, G., and Turner, J. S.: Turbulent gravitational convection from maintained and instantaneous sources, *Proc. R. Soc. Lond. A*, 234, 1–23, 1956.

Olbers, D. and Hellmer, H.: A box model of circulation and melting in ice shelf caverns, *Ocean Dynamics*, 60, 141–153, 2010.

15 Paolo, F. S., Fricker, H. A., and Padman, L.: Volume loss from Antarctic ice shelves is accelerating, *Science*, 348, 327–331, 2015.

Pollard, D. and DeConto, R. M.: Description of a hybrid ice sheet-shelf model, and application to Antarctica, *Geosci. Model Dev.*, 5, 1273–1295, 2012.

Pritchard, H. D., Arthern, R. J., Vaughan, D. G., and Edwards, L. A.: Extensive dynamic thinning on the margins of the Greenland and Antarctic ice sheets, *Nature*, 461, 971–975, 2009.

20 Pritchard, H. D., Ligtenberg, S. R. M., Fricker, H. A., Vaughan, D. G., Van den Broeke, M. R., and Padman, L.: Antarctic ice-sheet loss driven by basal melting of ice shelves, *Nature*, 484, 502–505, 2012.

Reerink, T. J., van de Berg, W. J., and van de Wal, R. S. W.: OBLIMAP 2.0: a fast climate model–ice sheet model coupler including online embeddable mapping routines, *Geosci. Model Dev.*, 9, 4111–4132, 2016.

Reese, R., Albrecht, T., Mengel, M., Asay-Davis, X., and Winkelmann, R.: Antarctic sub-shelf melt rates via PICO, *The Cryosphere Discuss.*, 25 pp. 1–24, doi:10.5194/tc-2017-70, 2017.

Rignot, E., Jacobs, S., Mouginot, J., and Scheuchl, B.: Ice-shelf melting around Antarctica, *Science*, 341, 266–270, 2013.

Ritz, C., Edwards, T. L., Durand, G., Payne, A. J., Peyaud, V., and Hindmarsh, R. C. A.: Potential sea-level rise from Antarctic ice-sheet instability constrained by observations, *Nature*, 528, 115–118, 2015.

Shabtaie, S. and Bentley, C. R.: West Antarctic ice streams draining into the Ross Ice Shelf: configuration and mass balance, *J. Geophys. Res. Solid Earth*, 92, 1311–1336, 1987.

30 Stern, A. A., Dinniman, M. S., Zagorodnov, V., Tyler, S. W., and Holland, D. M.: Intrusion of warm surface water beneath the McMurdo Ice Shelf, Antarctica, *J. Geophys. Res. Oceans*, 118, 7036–7048, 2013.